

Isogeometric Analysis with Geometrically Continuous Functions on Two-Patch Geometries

Mario Kapl^a, Vito Vitrih^b, Bert Jüttler^{a,*}, Katharina Birner^a

^a*Institute of Applied Geometry, Johannes Kepler University, Linz, Austria*

^b*IAM and FAMNIT, University of Primorska, Koper, Slovenia*

Abstract

We study the linear space of C^s -smooth isogeometric functions defined on a multi-patch domain $\Omega \subset \mathbb{R}^2$. We show that the construction of these functions is closely related to the concept of geometric continuity of surfaces, which has originated in geometric design. More precisely, the C^s -smoothness of isogeometric functions is found to be equivalent to geometric smoothness of the same order (G^s -smoothness) of their graph surfaces. This motivates us to call them C^s -smooth geometrically continuous isogeometric functions. We present a general framework to construct a basis and explore potential applications in isogeometric analysis. The space of C^1 -smooth geometrically continuous isogeometric functions on bilinearly parameterized two-patch domains is analyzed in more detail. Numerical experiments with bicubic and biquartic functions for performing L^2 approximation and for solving Poisson's equation and the biharmonic equation on two-patch geometries are presented and indicate optimal rates of convergence.

Keywords: Isogeometric Analysis, geometric continuity, geometrically continuous isogeometric functions, biharmonic equation, multi-patch domain

2000 MSC: 65D17, 65N30, 68U07

1. Introduction

In the framework of Isogeometric Analysis (IgA), which was introduced in [12], partial differential equations are discretized by using functions that are obtained from a parameterization of the computational domain. Typically one considers parameterizations by polynomial or rational spline functions (NURBS – non-uniform rational spline functions, see [20]) but other types of functions have been used also. On the one hand, this approach facilitates the data exchange with geometric design tools, since the mathematical technology used in Computer Aided Design (CAD) is based on parametric representations of curves and surfaces. On the other hand, it has been observed that the increased smoothness of the spline functions compared to traditional finite elements has a beneficial effect

*Corresponding author

Email addresses: `mario.kapl@jku.at` (Mario Kapl), `vito.vitrih@upr.si` (Vito Vitrih), `bert.juettler@jku.at` (Bert Jüttler), `k.birner@gmx.at` (Katharina Birner)

on stability and convergence properties [3, 9].

Clearly, regular single-patch NURBS parameterizations are available only for domains that are topologically equivalent to a box. Though it is possible to extend the applicability of such parameterizations slightly by considering parameterizations with singular points (cf. [27]), it is preferable to use other techniques, due to the difficulties introduced by the use of singularities.

One of the most promising approaches is to use multi-patch parameterizations, which are coupled across their interfaces. Several coupling techniques are available, such as the direct identification of the degrees of freedom along the boundaries as in [24], the use of Lagrangian multipliers as in [14], or Nitsche's method [17]. The approximation power of T-spline representations, which are a generalization of NURBS that allow T-junctions and extraordinary vertices in the mesh (cf. [26]), was explored for two-patch geometries in [2]. However, these multi-patch constructions in isogeometric analysis are limited to functions of low regularity (at most C^0 -smoothness). Consequently, the resulting numerical solutions are highly smooth almost everywhere, except across the interfaces between the patches of the multi-patch discretization.

Another approach is the use of trimmed NURBS geometries, which can also be combined with the multi-patch method. Such geometries have been used in the context of IgA (see e.g. [13, 21, 23]). However, trimming implies unavoidable gaps, when two trimmed NURBS patches are joined together (cf. [25]), and often requires advanced techniques for coupling the discretizations, see [21]. Another related technique is the use of mapped B-splines on general meshes [28].

The use of functions generated by subdivision algorithms has become a valuable alternative to NURBS, especially in Computer Graphics, since these functions lead to gap-free surfaces of arbitrary topology (cf. [19]). One of the standard subdivision methods is the Catmull-Clark subdivision, which generates surfaces consisting of bicubic patches, joined with C^2 -smoothness everywhere except at extraordinary vertices, where they have a well-defined tangent plane. A Catmull-Clark based isogeometric method for solids is presented in [7]. Disadvantages of using subdivision methods are the possible reduction of the approximation power in the vicinity of extraordinary vertices, cf. [16] and the need for special numerical integration techniques. In fact these functions are piecewise polynomial functions with an infinite number of segments.

Another possibility to deal with domains of general topology is the use of T-splines, which can represent more complex geometries. This has been exploited in IgA, see e.g. [1, 2]. However, the mathematical properties of the resulting isogeometric functions around the extraordinary vertices are not well understood. Around extraordinary vertices, T-splines are based on a special construction for geometrically continuous surfaces.

Geometric continuity is a well-known and highly useful concept in geometric design [18] and there exist numerous constructions for multi-patch surfaces with this property. It can be used to construct isogeometric functions of higher smoothness [4, 10], but the systematic exploration of the potential for IgA has just started. Numerical experiments with a multi-patch parameterization of a disk have been presented in [16]. The results indicate again a reduction of the approximation power (and consequently a lower order of convergence)

which is caused by the extraordinary vertices, similar to the case of subdivision algorithms.

Our paper consists of three main parts. Firstly we describe the concept of C^s -smooth geometrically continuous isogeometric functions on general multi-patch domains, and we present a general framework for computing a basis of the corresponding isogeometric discretization space in Section 2.

We then analyze the case of C^1 -smooth geometrically continuous functions on bilinearly parameterized two-patch domains in Section 3. The dimension of the space of these isogeometric functions is investigated and a particular selection of the basis is proposed. In addition, generalizations of our approach to more general two-patch domains are discussed.

Finally, in order to demonstrate the potential of geometric continuity for IgA, we present numerical experiments to explore the approximation power of C^1 -smooth geometrically continuous isogeometric functions for bilinearly parameterized two-patch geometries in Section 4. In addition to L^2 approximation and solving Poisson's equation, we also present results concerning the biharmonic equation, where the use of C^1 -smooth test functions greatly facilitates the (isogeometric) discretization. Our numerical results indicate that the geometrically continuous representations maintain the full approximation power. This may be due to the fact that the effect of geometric continuity in our approach is not restricted to the vicinity of an extraordinary vertex as in earlier approaches, but spread out along the entire interface between the patches.

2. Geometrically continuous isogeometric functions

We present the concept of geometrically continuous isogeometric functions on general multi-patch domains. We show that geometric continuity of graphs of isogeometric functions is equivalent to standard continuity of isogeometric functions. Furthermore, we present a general framework for computing a basis of the corresponding isogeometric space.

2.1. C^s -smooth isogeometric functions

In order to simplify the presentation we restrict ourselves to the case of two-dimensional computational domains. Given a positive integer n , we consider n bijective, regular geometry mappings

$$\mathbf{G}^{(\ell)} : [0, 1]^2 \rightarrow \mathbb{R}^2, \quad \ell \in \{1, \dots, n\},$$

which are represented in coordinates by

$$\boldsymbol{\xi}^{(\ell)} = (\xi_1^{(\ell)}, \xi_2^{(\ell)}) \mapsto (G_1^{(\ell)}, G_2^{(\ell)}) = \mathbf{G}^{(\ell)}(\boldsymbol{\xi}^{(\ell)}),$$

with $\mathbf{G}^{(\ell)} \in \mathcal{S}^{(\ell)} \times \mathcal{S}^{(\ell)}$, where $\mathcal{S}^{(\ell)}$ is a tensor-product NURBS space of degree $d_\ell \in \mathbb{N}_0^2$. Consequently, each geometry mapping $\mathbf{G}^{(\ell)}$, $\ell \in \{1, \dots, n\}$, is defined as a linear combination of NURBS basis functions $\psi_i^{(\ell)} : [0, 1]^2 \rightarrow \mathbb{R}$, i.e.,

$$\mathbf{G}^{(\ell)}(\boldsymbol{\xi}^{(\ell)}) = \sum_{i \in I_\ell} \mathbf{d}_i^{(\ell)} \psi_i^{(\ell)}(\boldsymbol{\xi}^{(\ell)}),$$

with a suitable index set I_ℓ (a box in index space) and control points $\mathbf{d}_i^{(\ell)} \in \mathbb{R}^2$. Thus it is a two-dimensional regular NURBS surface patch in \mathbb{R}^2 . More precisely, we even assume that the geometry mappings $\mathbf{G}^{(\ell)}$ are defined and regular on a neighborhood of $[0, 1]^2$.

Each geometry mapping $\mathbf{G}^{(\ell)}$, $\ell \in \{1, \dots, n\}$, defines a quadrilateral subdomain or *patch*

$$\Omega^{(\ell)} = \mathbf{G}^{(\ell)}([0, 1]^2).$$

We assume that the interiors of these subdomains are mutually disjoint, i.e.

$$\mathbf{G}^{(\ell)}((0, 1)^2) \cap \mathbf{G}^{(k)}((0, 1)^2) = \emptyset$$

for $\ell, k \in \{1, \dots, n\}$ with $\ell \neq k$. The computational domain $\Omega \subset \mathbb{R}^2$ is the union of these quadrilateral patches $\Omega^{(\ell)}$, i.e.,

$$\Omega = \bigcup_{\ell=1}^n \Omega^{(\ell)}.$$

On each patch $\Omega^{(\ell)}$, $\ell \in \{1, \dots, n\}$, the space of isogeometric functions is given by

$$\mathcal{S}^{(\ell)} \circ (\mathbf{G}^{(\ell)})^{-1}.$$

Given a positive integer s , which specifies the order of smoothness, the space

$$V = \left\{ v \in C^s(\Omega) : v|_{\Omega^{(\ell)}} \in \mathcal{S}^{(\ell)} \circ (\mathbf{G}^{(\ell)})^{-1} \text{ for all } \ell \in \{1, \dots, n\} \right\}$$

contains the *globally C^s -smooth isogeometric functions* defined on the computational domain Ω .

2.2. Geometric continuity of the graph surfaces

Let us consider an isogeometric function $w \in V$ in more detail. On each patch $\Omega^{(\ell)}$, $\ell \in \{1, \dots, n\}$, the function w is represented by

$$(w|_{\Omega^{(\ell)}})(\mathbf{x}) = w^{(\ell)}(\mathbf{x}) = \left(W^{(\ell)} \circ (\mathbf{G}^{(\ell)})^{-1} \right) (\mathbf{x}), \quad \mathbf{x} \in \Omega^{(\ell)}, \quad (1)$$

with $W^{(\ell)} \in \mathcal{S}^{(\ell)}$. Note the difference between $W^{(\ell)}$, which is a function defined on the local parameter domain $[0, 1]^2$, and $w^{(\ell)}$, which is the associated segment of the isogeometric function defined on $\Omega^{(\ell)}$.

The associated graph surface $\mathbf{F}^{(\ell)}$ of $w^{(\ell)}$ possesses the form

$$\mathbf{F}^{(\ell)}(\boldsymbol{\xi}^{(\ell)}) = \left(\underbrace{G_1^{(\ell)}(\boldsymbol{\xi}^{(\ell)}), G_2^{(\ell)}(\boldsymbol{\xi}^{(\ell)})}_{=\mathbf{G}^{(\ell)}(\boldsymbol{\xi}^{(\ell)})}, W^{(\ell)}(\boldsymbol{\xi}^{(\ell)}) \right)^T.$$

For any bivariate function f we denote with $\partial_i f$ its partial derivative with respect to the i -th argument. Depending on the domain of the function, this argument can be either one of the local parameters $\xi_i^{(\ell)}$ or one of the coordinates x_i in the physical domain.

We consider two neighboring patches $\Omega^{(\ell)}$ and $\Omega^{(k)}$ with the common interface $e^{(\ell k)} = \Omega^{(\ell)} \cap \Omega^{(k)}$, see Fig. 1. Since $w \in C^s(\Omega)$, the derivatives up to order s of the functions $w^{(\ell)}$ and $w^{(k)}$ at the common interface have to be equal, i.e.,

$$(\partial_1^i \partial_2^j w^{(\ell)})(\mathbf{x}) = (\partial_1^i \partial_2^j w^{(k)})(\mathbf{x}), \quad \mathbf{x} \in e^{(\ell k)}, \quad i + j \leq s, \quad (2)$$

where $\mathbf{x} = (x_1, x_2)$ are the global (world) coordinates with respect to the computational domain Ω . We evaluate the derivatives at the boundary of the patches by considering one-sided limits. Moreover we assume that the geometry mappings and their inverses are at least C^s -smooth.

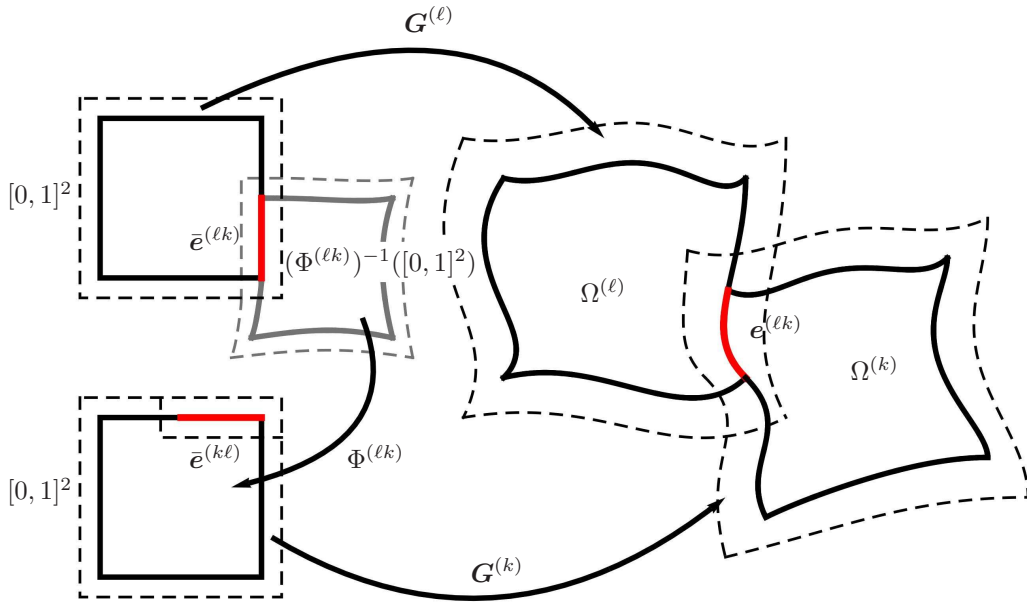


Figure 1: The geometry mappings $G^{(\ell)}$ and $G^{(k)}$ which are defined on a neighborhood of $[0, 1]^2$.

We may also parameterize the graph surfaces $F^{(\ell)}$ and $F^{(k)}$ with respect to the world coordinates x_1 and x_2 , simply as

$$(x_1, x_2, w^{(\ell)}(x_1, x_2))^T \quad \text{and} \quad (x_1, x_2, w^{(k)}(x_1, x_2))^T.$$

The fact that $w \in V$ is true if and only if these two parameterized surfaces are joined together with C^s -smoothness along $e^{(\ell k)}$. This is obvious for the first two coordinates, and it is implied by (2) for the third one.

Recall that two parametric surfaces are said to be joined together with *geometric smoothness of order s* if there exist reparameterizations (parameter transformations) that transform them into two parametric surfaces that are joined together with C^s smoothness [11, 18]. (Typically only a reparameterization of one of the two surfaces is considered, but

it is also possible to reparameterize both surfaces.) The two graph surfaces $\mathbf{F}^{(\ell)}$ and $\mathbf{F}^{(k)}$ satisfy the criterion of this definition. We thus obtain:

Theorem 1. *Let $w : \Omega \rightarrow \mathbb{R}$ be an isogeometric function, which is defined on patches $\Omega^{(\ell)}$, $\ell \in \{1, \dots, n\}$, by isogeometric functions $w^{(\ell)}$, given in (1). Then $w \in V$ if and only if for all neighboring patches $\Omega^{(\ell)}$ and $\Omega^{(k)}$, $\ell, k \in \{1, \dots, n\}$ with $\ell \neq k$, the associated graph surfaces $\mathbf{F}^{(\ell)}$ and $\mathbf{F}^{(k)}$ meet at the common interface with geometric continuity of order s .*

PROOF. It suffices to consider two neighboring patches as shown in Fig. 1. It has already been observed that the C^s -smoothness of w implies the geometric continuity of order s of the associated graph surfaces. We still need to prove the other implication. If the two surfaces meet with geometric continuity of order s then there exists a parameter transformation $\Phi^{(\ell k)}$ such that the two surfaces $\mathbf{F}^{(\ell)}$ and $\mathbf{F}^{(k)} \circ \Phi^{(\ell k)}$ meet with C^s -smoothness across the common interface, i.e., the composed surface patch

$$\mathbf{F}^+(\boldsymbol{\xi}^+) = \left(\underbrace{G_1^+(\boldsymbol{\xi}^+), G_2^+(\boldsymbol{\xi}^+)}_{=\mathbf{G}^+(\boldsymbol{\xi}^+)}, W^+(\boldsymbol{\xi}^+) \right)^T$$

which is defined on $[0, 1]^2 \cup (\Phi^{(\ell k)})^{-1}([0, 1]^2)$ by

$$\mathbf{F}^+(\boldsymbol{\xi}^+) = \begin{cases} \mathbf{F}^{(\ell)}(\boldsymbol{\xi}^+) & \text{if } \boldsymbol{\xi}^+ \in [0, 1]^2 \\ \mathbf{F}^{(k)}(\Phi^{(\ell k)}(\boldsymbol{\xi}^+)) & \text{if } \boldsymbol{\xi}^+ \in (\Phi^{(\ell k)})^{-1}([0, 1]^2) \end{cases}$$

is C^s -smooth. Consequently, the function $W^+ \circ (\mathbf{G}^+)^{-1}$ is also C^s -smooth. The fact that $w \in V$ then follows from $W^+ \circ (\mathbf{G}^+)^{-1}|_{\Omega^{(\ell)}} = w^{(\ell)}$ and $W^+ \circ (\mathbf{G}^+)^{-1}|_{\Omega^{(k)}} = w^{(k)}$. \square

Consequently, we will refer to the functions $w \in V$ as *C^s -smooth geometrically continuous isogeometric functions*. In fact, the functions themselves possess the standard smoothness properties, but their graph surfaces are joined with geometric continuity.

Theorem 1 is equivalent to a very recent result in [10], where the authors observed that *matched G^k -constructions always yield C^k -continuous isogeometric elements*. In contrast to that approach, which is based on the usual viewpoint in geometric design, we started our derivation from the given domain parameterization and not from the reparameterization $\Phi^{(\ell k)}$. We feel that this viewpoint fits better into the IGA framework, where the computational domain is central. It also leads to a natural framework for the construction of a basis of the space V . This is described in the next subsection.

2.3. Constructing a basis: General framework

Constructing a basis is an essential first step, which is required in order to use geometrically continuous isogeometric functions for simulations. We will construct isogeometric basis functions on Ω , which span the space V of all C^s -smooth geometrically continuous isogeometric functions. On each patch $\Omega^{(\ell)}$, $\ell \in \{1, 2, \dots, n\}$, any such basis function – which we again denote by w – is given by a representation of the form (1). According to Theorem 1, the functions w are C^s -smooth on Ω if and only if the graph surfaces join

with geometric smoothness of order s across the common interface $\mathbf{e}^{(\ell k)}$ for all neighboring patches $\Omega^{(\ell)}, \Omega^{(k)}$, $\ell, k \in \{1, 2, \dots, n\}$, with $\ell \neq k$.

We choose a basis $(\psi_j^{(\ell)})_{j \in I_\ell}$ for each local spline space $\mathcal{S}^{(\ell)}$, e.g., the NURBS basis functions on each patch. Consequently, the functions $W^{(\ell)} \in \mathcal{S}^{(\ell)}$, which define the basis function, have a local representation

$$W^{(\ell)}(\boldsymbol{\xi}^{(\ell)}) = \sum_{j \in I_\ell} b_j^{(\ell)} \psi_j^{(\ell)}(\boldsymbol{\xi}^{(\ell)}).$$

Using Eq. (1) and (2) we obtain constraints on their coefficients,

$$\sum_{j \in I_\ell} b_j^{(\ell)} (\partial_1^i \partial_2^j (\psi_j^{(\ell)} \circ (\mathbf{G}^{(\ell)})^{-1}))(\mathbf{x}) = \sum_{j \in I_k} b_j^{(k)} (\partial_1^i \partial_2^j (\psi_j^{(k)} \circ (\mathbf{G}^{(k)})^{-1}))(\mathbf{x}), \quad \mathbf{x} \in \mathbf{e}^{(\ell k)}.$$

Since we are considering a finite-dimensional space of functions, these constraints are equivalent to finitely many linear constraints on the coefficients $b_j^{(\ell)}$ and $b_j^{(k)}$, which can be formulated as a homogeneous linear system

$$H\mathbf{b} = 0, \quad \mathbf{b} = \left(b_j^{(\ell)} \right)_{j \in I_\ell, \ell \in \{1, 2, \dots, n\}}. \quad (3)$$

We now choose a basis of the null space (the kernel) of the matrix H . Each basis vector defines via (1) a function

$$W_i = (W_i^{(\ell)})_{\ell \in \{1, 2, \dots, n\}}, \quad i = 1, 2, \dots, \dim(\ker H).$$

Consequently, every function W_i then defines by (1) an isogeometric basis function

$$w_i = (w_i^{(\ell)})_{\ell \in \{1, 2, \dots, n\}} \in C^s(\Omega).$$

There are several possible strategies for choosing a basis of the null space of H . One may try to select basis functions with local supports and to avoid basis functions having large supports. Moreover, it is possible to extend the linear system (3) by adding further linear equations to satisfy certain conditions on the basis, e.g., homogeneous boundary conditions when solving Poisson's equation and the biharmonic equation (see Sections 4.3 and 4.4). The case of two patches will be studied in the next section.

3. C^1 -smooth functions on bilinear two-patch geometries

In this section, we restrict the order of continuity to $s = 1$ and consider two-patch configurations, where both patches are bilinearly parameterized, but represented as B-spline patches of degree (d, d) for $d \in \{3, 4\}$. First, the dimension of the resulting space V of the C^1 -smooth geometrically continuous isogeometric functions on such domains will be analyzed. Next, a basis of V will be presented, providing explicit formulas for $d = 4$. Finally, we discuss the generalization to more general two-patch domains.

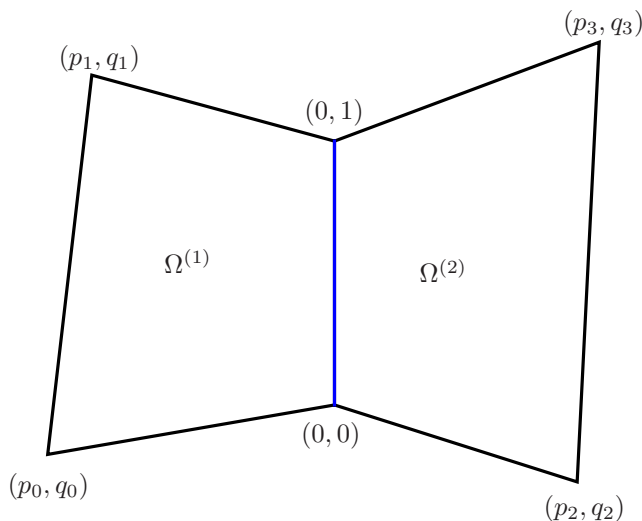


Figure 2: A two patch domain Ω consisting of two patches $\Omega^{(1)}$ and $\Omega^{(2)}$ that are defined by two bilinearly parameterized geometry mappings $\mathbf{G}^{(1)}$ and $\mathbf{G}^{(2)}$. These mappings are determined by the 6 patch vertices $(0, 0)$, $(0, 1)$, (p_0, q_0) , (p_1, q_1) , (p_2, q_2) and (p_3, q_3) .

3.1. Bilinearly parameterized two-patch domains

We assume that the domain Ω consists of two patches $\Omega^{(1)}$ and $\Omega^{(2)}$, i.e. $\Omega = \Omega^{(1)} \cup \Omega^{(2)}$, see Fig. 2, which are glued together in such a way that they share the whole common edge (shown in blue). We assume, that the two patches $\Omega^{(1)}$ and $\Omega^{(2)}$ are defined by two bilinear geometry mappings $\mathbf{G}^{(1)}$ and $\mathbf{G}^{(2)}$. The shape of the patches is determined by the 8 parameters p_i, q_i , $i = 0, \dots, 3$, which form the *shape vector* in \mathbb{R}^8 that characterizes the two-patch geometry. This vector is said to be *feasible* if the two patches are disjoint and the bilinear parameterizations are both regular on $[0, 1]^2$. The set \mathcal{F} of feasible shape vectors forms an open subset of \mathbb{R}^8 . Indeed, for any pair of regular parameterization, the determinants of the two Jacobians are strictly positive on $[0, 1]^2$, and this remains valid within a certain neighborhood of the associated shape vector in \mathbb{R}^8 .

The two bilinear patches are represented as B-spline patches of degree (d, d) that possess the knot vectors

$$\left(\underbrace{0, \dots, 0}_{d+1\text{-times}}, \underbrace{\frac{1}{k+1}, \dots, \frac{1}{k+1}}_{d-1\text{-times}}, \underbrace{\frac{2}{k+1}, \dots, \frac{2}{k+1}}_{d-1\text{-times}}, \dots, \underbrace{\frac{k}{k+1}, \dots, \frac{k}{k+1}}_{d-1\text{-times}}, \underbrace{1, \dots, 1}_{d+1\text{-times}} \right),$$

in both parameter directions, where $k \in \mathbb{N}_0$. Such B-spline patches are obtained by

1. parameterizing the domains $\Omega^{(1)}$ and $\Omega^{(2)}$ as bilinear Bézier patches,
2. applying degree-elevation $d - 1$ times, and
3. inserting k equidistant inner knots of multiplicity $d - 1$ in both parameter directions.

This construction guarantees that the common edge

$$\mathbf{G}^{(1)}(1, \xi) = \mathbf{G}^{(2)}(0, \xi), \quad \xi = \xi_2^{(1)} = \xi_2^{(2)} \in [0, 1], \quad (4)$$

is parameterized identically by both patches. Consequently, an isogeometric function w is continuous (C^0 -smooth) across this edge if and only if

$$W^{(1)}(1, \xi) = W^{(2)}(0, \xi). \quad (5)$$

Let us now consider the tangent planes of the two graph surfaces $\mathbf{F}^{(1)}$ and $\mathbf{F}^{(2)}$ at the points of the common edge. They are spanned by the derivative vectors

$$\partial_1 \mathbf{F}^{(1)}(1, \xi), \partial_2 \mathbf{F}^{(1)}(1, \xi) \text{ and } \partial_1 \mathbf{F}^{(2)}(0, \xi), \partial_2 \mathbf{F}^{(2)}(0, \xi),$$

respectively. The C^1 -smoothness of the isogeometric function w is guaranteed if the 3×4 matrix formed by them has rank 2 only, since then the two tangent planes at any point $\mathbf{G}^{(1)}(1, \xi)$ are identical. Due to the identity

$$\partial_2 \mathbf{F}^{(1)}(1, \xi) = \partial_2 \mathbf{F}^{(2)}(0, \xi),$$

which is implied by the continuity conditions (4) and (5), this is equivalent to

$$\det \left((\partial_1 \mathbf{F}^{(1)})(1, \xi), (\partial_1 \mathbf{F}^{(2)})(0, \xi), (\partial_2 \mathbf{F}^{(2)})(0, \xi) \right) = 0, \quad \xi \in [0, 1], \quad (6)$$

which is a well-known condition for first order geometric continuity between two surface patches, cf. [11]. This condition leads us to the homogeneous linear system (3) for the coefficients $b_j^{(1)}$ and $b_j^{(2)}$ of the function $W^{(1)}$ and $W^{(2)}$, respectively.

The basis of V consists of two different kinds of C^1 -smooth geometrically continuous isogeometric functions. The *basis functions of the first kind* possess a support that is contained in one of the two patches only. We consider the functions that are obtained by composing a tensor-product B-spline on one of the patches with the inverse geometry mappings,

$$\mathbf{x} \mapsto \begin{cases} (\psi_i^{(\ell)} \circ (\mathbf{G}^{(\ell)})^{-1})(\mathbf{x}) & \text{if } \mathbf{x} \in \Omega^{(\ell)} \\ 0 & \text{otherwise} \end{cases} \quad \ell \in \{1, 2\}, \quad (7)$$

where neither the support of the B-spline $\psi_i^{(\ell)}$ nor of its first derivatives intersect the interface with the other patch. These functions have exactly one non-zero coefficient $b_j^{(\ell)}$.

All coefficients $b_j^{(\ell)}$ that correspond to the control points of the common edge or one of the neighboring columns of the two patches $\mathbf{G}^{(1)}$ and $\mathbf{G}^{(2)}$, are always zero. Therefore, the number of these functions is equal to

$$2(d - 1 + k(d - 1))(d + 1 + k(d - 1)). \quad (8)$$

Note that the coefficients $b_j^{(\ell)}$ of these isogeometric functions are independent of the geometry mappings.

In contrast, the *basis functions of the second kind* depend on the geometry mappings. Here, the coefficients $b_{j,i}^{(\ell)}$ of the functions that do not correspond to the control points of the common edge or one of the neighboring columns of the two B-spline patches are set to zero. We have to choose suitable coefficients for the remaining $(d + 1 + k(d - 1))$ coefficients in order to obtain functions that are C^1 -smooth across the interface. The number of these functions will be analyzed in the following section.

3.2. Dimension of the space

We investigate the dimension of the space V of C^1 -smooth geometrically continuous isogeometric functions on the above described bilinearly parameterized two-patch domains. Recall that the number of functions of the first kind can be computed with help of formula (8). It remains to analyze the number of linearly independent functions of the second kind.

Expanding the determinant in (6) gives

$$\gamma(\xi)y(\xi) = \alpha(\xi)r(\xi) + \beta(\xi)t(\xi), \quad \xi \in [0, 1], \quad (9)$$

where

$$r(\xi) = \partial_2 W^{(1)}(1, \xi) = \partial_2 W^{(2)}(0, \xi), \quad t(\xi) = \partial_1 W^{(1)}(1, \xi) \text{ and } y(\xi) = \partial_1 W^{(2)}(0, \xi)$$

with the coefficient functions

$$\begin{aligned} \alpha(\xi) &= \partial_1 G_1^{(2)}(0, \xi) \partial_1 G_2^{(1)}(1, \xi) - \partial_1 G_1^{(1)}(1, \xi) \partial_1 G_2^{(2)}(0, \xi), \\ \beta(\xi) &= \partial_2 G_1^{(1)}(1, \xi) \partial_1 G_2^{(2)}(0, \xi) - \partial_1 G_1^{(2)}(0, \xi) \partial_2 G_2^{(1)}(1, \xi), \\ \gamma(\xi) &= \partial_2 G_1^{(1)}(1, \xi) \partial_1 G_2^{(1)}(1, \xi) - \partial_1 G_1^{(1)}(1, \xi) \partial_2 G_2^{(1)}(1, \xi). \end{aligned}$$

The coefficient functions α , β and γ are polynomials of degree 2, 1 and 1, respectively.

Eq. (9) leads to the following interesting observation. Since the functions t and y as well as the coefficient functions are C^1 -smooth, the function r has to be C^1 -smooth whenever $\alpha(\xi) \neq 0$ holds. This is in contrast to the case $\alpha(\xi) = 0$, which includes the C^1 -joint of two graph surfaces, where C^0 -smoothness of the function r is sufficient.

Let us denote by \mathbb{S}_k^d the C^1 -smooth spline space of degree d in $[0, 1]$ with k uniform inner knots. Then the inner knots possess multiplicity $d-1$ to characterize C^1 -smoothness. We are interested in solutions

$$(r, t, y) \in \mathbb{S}_k^{d-1} \times \mathbb{S}_k^d \times \mathbb{S}_k^d$$

of Eq. (9). These solutions form a linear space L .

The following lemma analyzes the dimension $\dim L$ for the case $k = 0$ in the *generic case*. More precisely, it applies when choosing a shape vector satisfying $\alpha(i/(k+1)) \neq 0$ for $i = 1, \dots, k$ and

$$p_1 p_2 \neq p_0 p_3. \quad (10)$$

The set of all feasible shape vectors satisfying this condition¹ is denoted by \mathcal{F}^* . It is an open subset of \mathcal{F} and also dense in \mathcal{F} .

Lemma 2. *If $k = 0$, then the dimension of L is equal to $2d$ in the generic case.*

¹In a slightly different setting a similar condition was also formulated in [4, Definition 17].

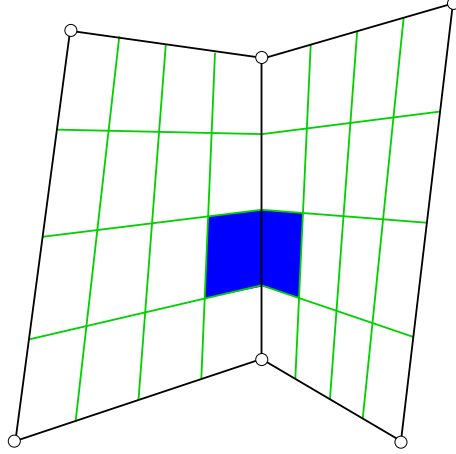


Figure 3: If two bilinear patches satisfy the genericity condition (10), then this condition is also satisfied by any pair of patches along the interface that is generated by the knot insertion.

PROOF. We consider Eq. (9) in more detail. This equation is equivalent to a homogeneous linear system

$$T\tilde{\mathbf{b}} = 0,$$

where $\tilde{\mathbf{b}}$ is the vector of the $3d + 2$ coefficients of the three functions r, t, y . Since both sides of (9) are polynomials of degree $d + 1$ we obtain a system consisting of $d + 2$ equations. Consequently, the space of solutions has at least dimension $3d + 2 - (d + 2) = 2d$.

The dimension of L exceeds $2d$ only if all $(d + 2) \times (d + 2)$ -submatrices of T are singular. Analyzing these determinants for $d = 3, 4$ confirms that at least one regular submatrix exists if the genericity condition (10) is satisfied. \square

The dimension of L in the non-generic case can take several values, depending on the specific configuration. A complete analysis of these situations is beyond the scope of the present paper, since this would require to analyze a large number of particular configurations. In a different setting, a similar discussion has been given in the recent manuscript [4].

We use this result to compute the dimension of L for general values of k .

Lemma 3. *The dimension of L is equal to $2d + k(2d - 4)$ in the generic case.*

PROOF. Consider a solution (r, t, y) of Eq. (9) in the generic case. Each pair of adjacent spline segments of the two patches along the interface can be seen as an instance of a configuration without inner knots ($k = 0$), see Fig. 3. A short computation confirms that all these pairs are again characterized by generic shape vectors if they are derived from a global generic one.

Consequently we can apply the previous lemma to each pair of patches. Thus, within each knot span $[\frac{i}{k+1}, \frac{i+1}{k+1}]$, $i \in \{0, \dots, k\}$, we represent the functions (r, t, y) with respect to some basis of this local space, using $2d(k + 1)$ coefficients.

In addition, the solution needs to satisfy C^1 -smoothness conditions at all knots. For this it suffices to consider the first two components (r, t) only since their values uniquely

determine the third one via (9). The C^1 -conditions between neighboring knot spans give a homogeneous linear system consisting of $4k$ equations.

In the generic case, these equations are linearly independent, since the functions r and t can interpolate any first-order Hermite data (i.e., function values and first derivatives) at all points in the interior of the domain. Indeed, the 4 triplets of functions $(r, t, y) \in L$,

$$\begin{aligned} (\gamma(\xi)\xi^i, 0, \alpha(\xi)\xi^i), & \quad i = 0, 1; \\ (0, \gamma(\xi)\xi^i, \beta(\xi)\xi^i), & \quad i = 0, 1; \end{aligned} \quad (11)$$

are linearly independent and can be extended to a basis of L . These four functions (11) can interpolate any first order Hermite data at all points satisfying $\gamma(\xi_0) \neq 0$. The violation of this condition causes the geometry mapping $G^{(1)}$ to be singular at $(1, \xi_0)$, cf. (9), while regularity of the mapping is always assumed.

This confirms that the $4k$ equations for C^1 -smoothness are linearly independent, hence the dimension of L is equal to $2d(k+1) - 4k$. \square

The number of linearly independent functions of the second kind is equal to $\dim L + 1$ since they can be obtained by integration from r, t and y . The additional degree of freedom is the integration constant. In fact, for each triplet $(r, t, y) \in L$ and integration constant C we obtain an isogeometric function of the second kind by evaluating the expressions

$$\begin{aligned} W^{(1)}(\xi_1^{(1)}, \xi_2^{(1)}) &= \int_0^{\xi_2^{(1)}} r(\zeta) d\zeta + (\xi_1^{(1)} - 1)t(\xi_2^{(1)}) + C, \\ W^{(2)}(\xi_1^{(2)}, \xi_2^{(2)}) &= \int_0^{\xi_2^{(2)}} r(\zeta) d\zeta + \xi_1^{(2)}y(\xi_2^{(2)}) + C. \end{aligned} \quad (12)$$

and subsequently eliminating the contributions of the functions of the first kind. More precisely, we express the functions defined by these formulas in the B-spline basis and replace the B-spline coefficients that are not located on the interface or in the neighboring column with zeros. Any basis function of the second kind is uniquely characterized by the triplet $(r, t, y) \in L$ and the integration constant C in (12).

It should be noted that the basis functions of the second kind (and consequently all functions in V) are C^2 -smooth along the common interface in the generic case, since r has to be C^1 -smooth. This is different from the case of C^1 -joint between the two patches, where the functions are only required to be C^1 -smooth along the common interface.

Theorem 4. *In the generic case the dimension of the space of C^1 -smooth geometrically continuous isogeometric functions on bilinear two-patch domains is equal to*

$$\dim V = \underbrace{2(d-1+k(d-1))(d+1+k(d-1))}_{\text{first kind}} + \underbrace{(2d+1) + (2d-4)k}_{\text{second kind}}.$$

PROOF. The space V is the direct sum of the linear spaces spanned by the basis functions of the first and second kind, as these two spaces have only the null function in common. Indeed, any function $f \in V$ has a unique decomposition into a linear combination of basis

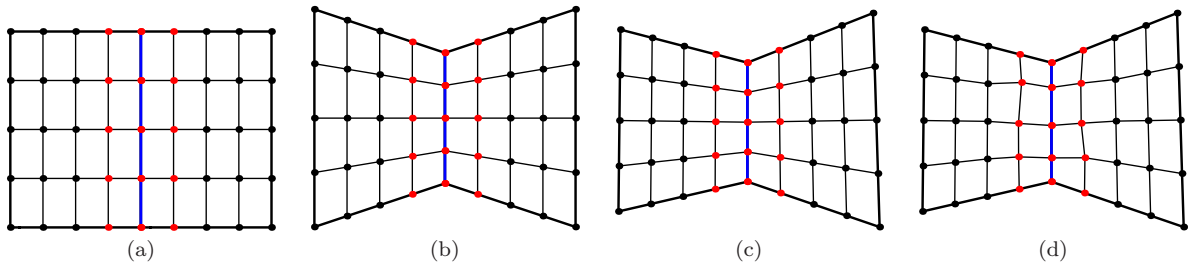


Figure 4: Different two-patch domains which are defined by two biquartic Bézier patches $\mathbf{G}^{(1)}$ and $\mathbf{G}^{(2)}$. The blue edge is the common edge of both patches. Only the red control points influence the dimension. The black ones can be chosen arbitrarily.

k	Domain (a)	Domain (b)	Domain (c)	Domain (d)
0	10	10	9	3
1	16	16	13	3
2	22	21	17	3
3	28	26	21	3
$k \geq 1$	$10 + 6k$	$11 + 5k$	$9 + 4k$	3

Table 1: The number of linearly independent C^1 -smooth geometrically continuous isogeometric basis functions of the second kind for some particular values of k for the domains shown in Fig. 4.

functions of the first kind (defined by all B-spline coefficients that are not located on the interface or in the neighboring column) and a function of the second kind, which is defined by the remainder. Since any basis function of the second kind is uniquely characterized by the triplet $(r, t, y) \in L$ and the integration constant C in (12) we may complete the proof using Lemma 3 and Eq. (8). \square

We present an example that shows how the number of linearly independent functions of the second kind is influenced by the geometry of the two-patch domains for $d = 4$.

Example 5. Let $d = 4$ and let us consider four different pairs of geometry mappings $\mathbf{G}^{(1)}$ and $\mathbf{G}^{(2)}$, which define computational domains Ω consisting of two quadrilateral patches $\Omega^{(1)}$ and $\Omega^{(2)}$, see Fig. 4. The domains (a) and (b) consist of two symmetric rectangles and trapezoids, respectively, which is in contrast to the domain (c), where the patches are not symmetric. Finally, the domain (d) is represented by a non-bilinear parameterization.

For all instances (a)-(d) we obtain a different number of linearly independent functions of the second kind. This number depends on the shape vector and is presented in Table 1. We explicitly computed the number of these functions for several small values of k and used these results to formulate conjectures for general values of k . The case (c) confirms Theorem 4, which applies to the generic case, whereas case (a) is well known since it exactly describes the C^1 -joint of two graph surfaces. It should be noted that non-bilinearly parameterized domains may give only 3 functions (corresponding to the linear polynomials on the domain) of the second kind, independently of the number of knots k .

In all cases, the dimension of V depends solely on the location of the red control points. The remaining ones can be replaced without changing the number of linearly independent functions of the first or second kind. \diamond

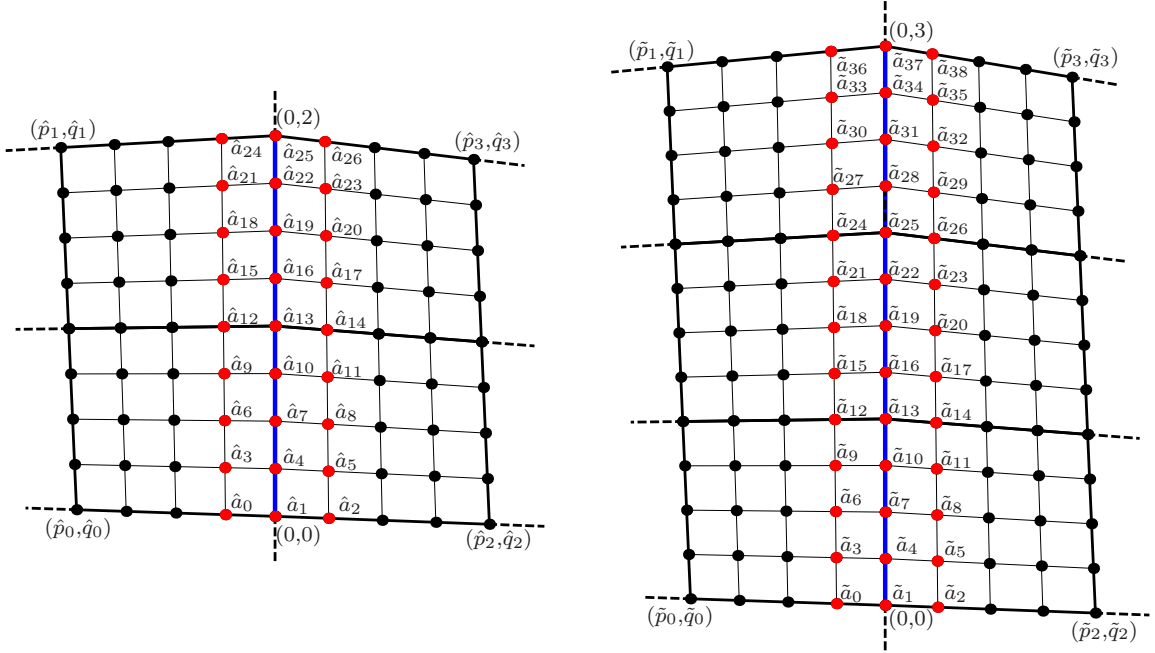


Figure 5: Bézier coefficients for two (left) and three (right) neighboring pairs of spline segments of $W^{(1)}$ and $W^{(2)}$ along the associated common interface of the two patches. The geometry of these configurations is specified by the points (\hat{p}_i, \hat{q}_i) and $(\tilde{p}_i, \tilde{q}_i)$, $i = 0, \dots, 3$. The formulas in the appendix refer to these configurations.

3.3. Basis of the space

We will describe the construction of a basis of the space V of C^1 -smooth geometrically continuous isogeometric functions on the above described bilinearly parameterized two-patch domains in more detail. As already explained in Section 3.1 our basis consists of two different kinds of functions. The construction of the functions of the first kind have been already described in (7). Now we focus on the functions of the second kind.

Our construction uses the Bézier representation of the $k + 1$ pairs of spline segments of $W^{(1)}$ and $W^{(2)}$ along the associated common interface of the B-spline patches $\mathbf{G}^{(1)}$ and $\mathbf{G}^{(2)}$. Since we consider only functions of the second kind only the Bézier coefficients along the common edge and in the neighboring columns are non-zero.

We will denote these Bézier coefficients by a_i and will identify the coefficients along the common edge, thereby ensuring continuity. In total we obtain $3d(k + 1) + 3$ coefficients a_i which will be used in the construction. These coefficients are numbered from bottom to top along the common interface. Fig. 5 shows examples of two and three pairs of neighboring spline segments, where the coefficients are denoted by \hat{a}_i and \tilde{a}_i , respectively. We introduced these additional variables in order to identify the coefficients in these special cases, which serve as masks for the general one.

As observed in the previous subsection, we obtain $d + 2$ linear equations for each pair of Bézier elements to achieve C^1 -smoothness of the isogeometric functions along the common interface. Ensuring C^1 -smoothness across inner knots of the patches requires $3k$ additional

equations. We arrive at a linear system

$$\tilde{H} \mathbf{a} = 0, \quad \mathbf{a} = (a_i)_{i \in \{0, \dots, 3d(k+1)+2\}}, \quad (13)$$

similar to (3). Note that not all equations are linearly independent. Selecting a basis of the nullspace of the matrix \tilde{H} gives the coefficients of the basis functions of the second kind.

We devised a procedure that creates a matrix which is as banded as possible and whose columns form a basis of the null space for the degrees $d = 3$ and $d = 4$ considered in this paper. The details of this method are described in [5]. This procedure revealed a pattern of basis functions that allowed us to derive simple explicit formulas for the basis functions of the second kind. In a subsequent step these formulas have been confirmed using symbolic computation.

The appendix reports the resulting Bézier coefficients for degree $d = 4$ in the generic case. (Similar formulas, not reported here due to space limitations, are available for $d = 3$ also.) We obtain four types of basis functions, see Fig. 6. The formulas in the appendix specify the values of the coefficients with respect to the local geometry of the bilinear two-patch configuration consisting of either two (types A, L, U) or three (type B) pairs of neighboring spline segments, see Fig. 5. We use the tilde $\tilde{\cdot}$ and the hat $\hat{\cdot}$ symbol to identify the local shape parameters (p_i, q_i) and the corresponding Bézier coefficients a_i . The classification of these functions is based on their support:

- A These basis functions are defined on two pairs of neighboring spline segments. There are three subtypes A.1-A.3. The total number of these functions is $3k$.
- B These basis functions are defined on three pairs of neighboring spline segments. There is only one subtype. The total number of these functions is $k - 1$.
- L These five basis functions (subtypes L.1-L.5), which are present at the lower boundary of the common interface, are defined on the first pair or the first two pairs of neighboring spline segments.
- U These five basis functions (subtypes U.1-U.5), which are present at the upper boundary of the common interface, are defined on the last pair or the last two pairs of neighboring spline segments.

It should be noted that all these basis functions are well defined for *any* generic configuration. They are even well-behaved in the vicinity of non-generic configurations and their coefficients are defined for any pair of regular bilinear patches.

We summarize our construction.

Theorem 6. *Let $d = 4$ and $k \geq 1$. The $9 + 4k$ basis functions of types A, B, L, U (see appendix and Fig. 5) combined with the basis functions of the first kind defined in (7) form a basis of the space V of C^1 -smooth geometrically continuous isogeometric functions in the generic case.*

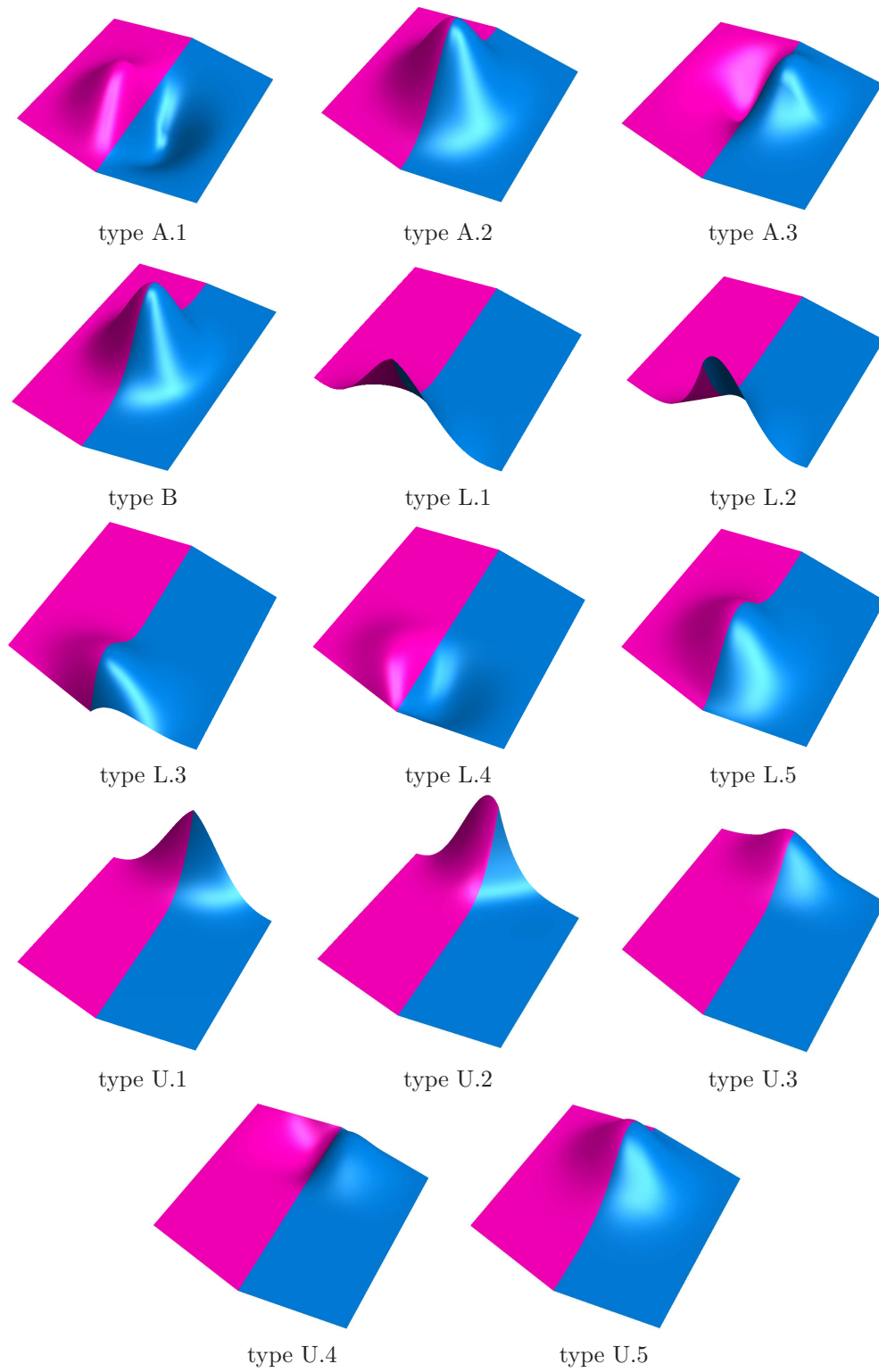


Figure 6: All different types of basis functions of the second kind for $d = 4$ (differently colored on the two patches Ω^1 and Ω^2). The formulas for the coefficients of these functions are given in the appendix.

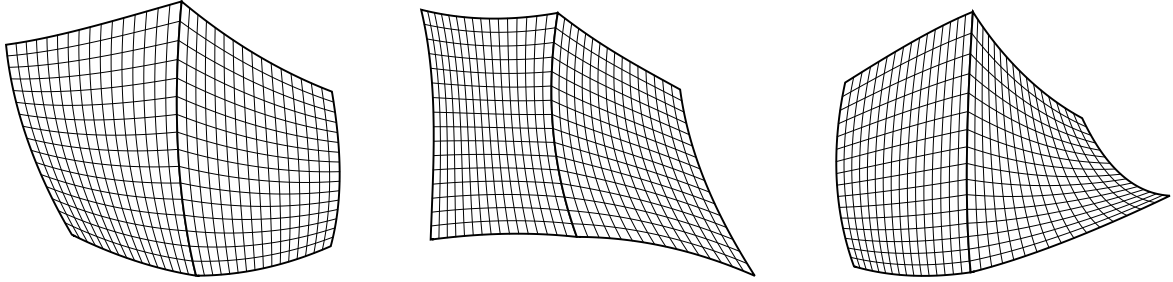


Figure 7: Three examples of two-patch domains Ω , where the common interfaces are not straight lines. Each domain is defined by geometry mappings $\mathbf{G}^{(1)}$ and $\mathbf{G}^{(2)}$, such that the two-dimensional surface patch consisting of $\mathbf{G}^{(1)}$ and $\mathbf{G}^{(2)}$ belongs to the space $V \times V$, where V is the space of C^1 -smooth geometrically continuous isogeometric functions on the domain from Fig. 8(a). Note that for each domain Ω the resulting space of C^1 -smooth geometrically continuous isogeometric functions has at least the same dimension as V .

PROOF. The use of symbolic computation confirms that the coefficient vectors solve the homogeneous linear system (13). The analysis of the coefficients of these vectors proves linear independence in the generic case. Finally, the number of these functions plus the number of basis functions of the first kind equals the dimension of the space V . \square

3.4. Beyond bilinear parameterizations

We describe two possible generalizations of our construction to more general two-patch domains.

Modification of certain control points of the geometry mappings $\mathbf{G}^{(1)}$ and $\mathbf{G}^{(2)}$. As described in Section 3.1 only the basis functions of the second kind depend on the initial geometry. Therefore, we can modify all control points of the bilinear geometry mappings $\mathbf{G}^{(1)}$ and $\mathbf{G}^{(2)}$ (represented as B-spline patches), which do not affect the basis functions of the second kind. More precisely, only the control points of the common interface and of the neighboring columns of the two splines patches $\mathbf{G}^{(1)}$ and $\mathbf{G}^{(2)}$ have to be kept (i.e., they have to comply with bilinear parameterizations) while the remaining control points can be modified. This allows us to construct C^1 -smooth geometrically continuous isogeometric functions on this particular class of two-patch domains that can have curved boundaries. However, the common interface of the two-patch domain needs to be a straight line. An example of a two-patch domain Ω , which can be parameterized by such geometry mappings $\mathbf{G}^{(1)}$ and $\mathbf{G}^{(2)}$, is visualized in Fig. 8(c).

Use of the space $V \times V$ to construct geometry mappings $\mathbf{G}^{(1)}$ and $\mathbf{G}^{(2)}$. Let \mathbf{G} be the two-dimensional surface patch which consists of the geometry mappings $\mathbf{G}^{(1)}$ and $\mathbf{G}^{(2)}$. By choosing geometry mappings $\mathbf{G}^{(1)}$ and $\mathbf{G}^{(2)}$ such that $\mathbf{G} \in V \times V$, we can define a more general two-patch domain Ω , for which the resulting space of C^1 -smooth geometrically continuous isogeometric functions possesses at least the same dimension as V . In contrast to the first strategy, this approach allows us to obtain C^1 -smooth geometrically continuous isogeometric functions on two-patch domains, where the common interfaces between the two patches are not necessarily straight lines, see Fig. 7.

4. Numerical results

We generate sequences of nested spaces of C^1 -smooth geometrically continuous isogeometric functions and use them for numerical experiments with L^2 approximation, Poisson's equation and the biharmonic equation.

4.1. Nested spaces of C^1 -smooth geometrically continuous isogeometric functions

Let $\Omega = \Omega^{(1)} \cup \Omega^{(2)}$ be a general two-patch domain defined by two bilinear geometry mappings $\mathbf{G}^{(1)}$ and $\mathbf{G}^{(2)}$ which are represented as bicubic ($d = 3$) or biquartic ($d = 4$) patches using degree elevation. Some of the control points (sufficiently far away from the interface) are further modified in order to obtain more general geometries (see Section 3.4).

We first construct C^1 -smooth geometrically continuous isogeometric basis functions as described in Section 3. Further, in order to obtain a finer space, we insert $2^L - 1$, $L \in \mathbb{N}$, equidistant inner knots of multiplicity $d - 1$ in both parameter directions, where L is the *level of the refinement*. This gives C^1 -smooth geometrically continuous isogeometric basis functions for a refined space, which will be denoted by V_h , where $h = \mathcal{O}(2^{-L})$. The geometrically continuous isogeometric functions are globally C^1 -smooth and piecewise C^∞ -smooth, and therefore belong to the space $H^2(\Omega)$. Since all functions $v' \in V_{h'}$ can be represented as linear combinations of functions $v \in V_h$ for $h \leq h'$, we get a sequence of nested spaces $V_h \subset H^2(\Omega)$.

Later, for solving Poisson's equation and the biharmonic equation, respectively, we will need C^1 -smooth geometrically continuous isogeometric functions w_i , which satisfy the boundary conditions

$$w_i(\mathbf{x}) = 0 \text{ on } \partial\Omega$$

and

$$w_i(\mathbf{x}) = \frac{\partial w_i}{\partial \mathbf{n}}(\mathbf{x}) = 0 \text{ on } \partial\Omega,$$

respectively. We obtain sequences of nested spaces by solving the linear system (3) with additional linear equations for the corresponding boundary conditions. These spaces will be denoted by $V_{0,0h}$ and $V_{1,0h}$, respectively.

For $d = 4$, in addition to the suitable basis functions of the first kind, the space $V_{0,0h}$ is spanned by all functions of types A.1, A.2, A.3, B, L.4, L.5, U.4 and U.5, and the space $V_{1,0h}$ is spanned by all functions of types A.1, A.2, A.3 and B.

Example 7. We consider the three different computational domains Ω , shown in Fig. 8 (first row), which consist of two quadrilateral patches $\Omega^{(1)}$ and $\Omega^{(2)}$. For the domains (a) and (b), the corresponding initial geometry mappings $\mathbf{G}^{(1)}$ and $\mathbf{G}^{(2)}$ are bilinear parameterizations, which are represented as Bézier patches of degree (d, d) for $d = 3, 4$. In case of domain (c), the initial geometry mappings $\mathbf{G}^{(1)}$ and $\mathbf{G}^{(2)}$ are again Bézier patches of degree (d, d) for $d = 3, 4$, but they are chosen in such a way that the control points of the common edge and of the first neighboring columns are a part of a bilinear parameterization. In addition, the figure also shows the different exact analytic solutions, which will be used in the remaining examples in this section to verify the order of convergence.

Table 2 reports the number of isogeometric basis functions for various levels L of refinement and for the different boundary conditions. \diamond

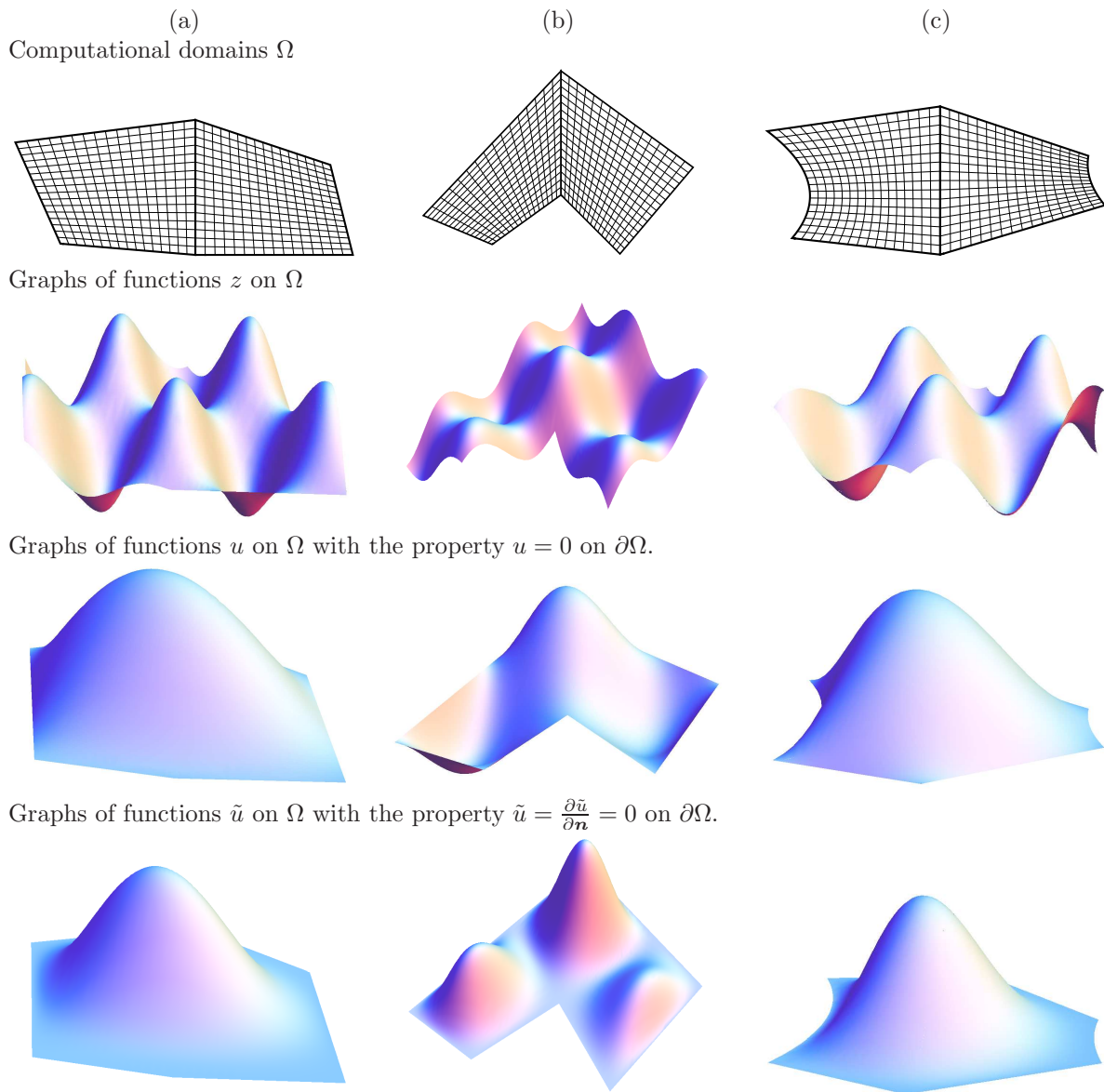


Figure 8: Three different two-patch domains Ω (first row) on which different functions are defined, which are to be approximated by L^2 norm minimization (second row) in Example 8, or used as exact solutions (third row) for Poisson's equation in Example 9, or as exact solutions (fourth row) for the biharmonic equation in Example 10.

In the following subsections we present three possible applications of these isogeometric functions over two-patch domains, in order to demonstrate their potential for IgA on the basis of several examples.

4.2. L^2 approximation

Let $z : \Omega \rightarrow \mathbb{R}$ be a smooth function defined on a two-patch domain $\Omega = \Omega^{(1)} \cup \Omega^{(2)}$. In addition, let $\{w_i\}_{i \in I}$ for $I = \{1, 2, \dots, \dim V_h\}$ be a set of C^1 -smooth geometrically

b.c.		L^2 approximation				Poisson's equation				Biharmonic equation			
		Bicubic		Biquartic		Bicubic		Biquartic		Bicubic		Biquartic	
L	# patches	# bfct	# k2	# bfct	# k2	# bfct	# k2	# bfct	# k2	# bfct	# k2	# bfct	# k2
0	2	23	7	39	9	5	1	15	3	-	-	-	-
1	8	57	9	109	13	27	3	67	7	-	-	35	3
2	32	173	13	357	21	119	7	279	15	75	3	211	11
3	128	597	21	1285	37	495	15	1135	31	403	11	995	27
4	512	2213	37	4869	69	2015	31	4575	63	1827	27	4291	59
5	2048	8517	69	19849	133	8127	63	18367	127	7747	59	17795	123

Table 2: The number of C^1 -smooth geometrically continuous isogeometric basis functions (# bfct: in total, # k2: second kind) for each level L for the three domains in Fig. 10 without boundary conditions (for L^2 approximation) and with homogeneous boundary conditions of order 0 and 1 (for Poisson's equation and for the biharmonic equation).

continuous isogeometric functions, which form a basis of a subspace V_h of $H^2(\Omega)$. We approximate the function z by the function

$$u_h(\mathbf{x}) = \sum_{i \in I} c_i w_i(\mathbf{x}), \quad c_i \in \mathbb{R},$$

using the least squares approach, i.e., we compute the coefficients $\{c_i\}_{i \in I}$ such that

$$\|u_h - z\|_0^2 = \int_{\Omega} (u_h(\mathbf{x}) - z(\mathbf{x}))^2 d\mathbf{x} \rightarrow \min_{c_i, i \in I}. \quad (14)$$

The minimization problem (14) can be formulated as a system of linear equations $K\mathbf{c} = \mathbf{z}$ for the unknown coefficients $\mathbf{c} = (c_i)_{i \in I}$, where the elements of the (mass) matrix $K = (k_{i,j})_{i,j \in I}$ and of the vector $\mathbf{z} = (z_i)_{i \in I}$ are

$$k_{i,j} = \int_{\Omega} w_i(\mathbf{x}) w_j(\mathbf{x}) d\mathbf{x} \quad \text{and} \quad z_i = \int_{\Omega} z(\mathbf{x}) w_i(\mathbf{x}) d\mathbf{x}.$$

Since the functions w_i are given as in (1) the entries $k_{i,j}$ and z_i can be rewritten as

$$k_{i,j} = k_{i,j}^{(1)} + k_{i,j}^{(2)}, \quad k_{i,j}^{(\ell)} = \int_{[0,1]^2} W_i^{(\ell)}(\boldsymbol{\xi}^{(\ell)}) W_j^{(\ell)}(\boldsymbol{\xi}^{(\ell)}) |\det J^{(\ell)}(\boldsymbol{\xi}^{(\ell)})| d\boldsymbol{\xi}^{(\ell)}, \quad \ell = 1, 2,$$

and

$$z_i = z_i^{(1)} + z_i^{(2)}, \quad z_i^{(\ell)} = \int_{[0,1]^2} z(\mathbf{G}^{(\ell)}(\boldsymbol{\xi}^{(\ell)})) W_i^{(\ell)}(\boldsymbol{\xi}^{(\ell)}) |\det J^{(\ell)}(\boldsymbol{\xi}^{(\ell)})| d\boldsymbol{\xi}^{(\ell)}, \quad \ell = 1, 2,$$

where $J^{(\ell)}$ is the Jacobian of $\mathbf{G}^{(\ell)}$.

Example 8. We use the isogeometric basis functions on the three domains described in the previous example to apply L^2 approximation to smooth functions, which are defined on the domains (a)-(c).

More precisely, we approximate for all three domains the same function

$$z(x_1, x_2) = 2 \cos(2x_1) \sin(2x_2), \quad (15)$$

L	Bicubic						Biquartic					
	Domain (a)		Domain (b)		Domain (c)		Domain (a)		Domain (b)		Domain (c)	
	$\frac{\ z-u_h\ _0}{\ z\ _0}$	c.r. $\ \cdot\ _0$	$\frac{\ z-u_h\ _0}{\ z\ _0}$	c.r. $\ \cdot\ _0$	$\frac{\ z-u_h\ _0}{\ z\ _0}$	c.r. $\ \cdot\ _0$	$\frac{\ z-u_h\ _0}{\ z\ _0}$	c.r. $\ \cdot\ _0$	$\frac{\ z-u_h\ _0}{\ z\ _0}$	c.r. $\ \cdot\ _0$	$\frac{\ z-u_h\ _0}{\ z\ _0}$	c.r. $\ \cdot\ _0$
0	0.62276	-	0.60175	-	0.44238	-	0.09259	-	0.36954	-	0.09068	-
1	0.05315	3.5505	0.18912	1.67	0.04593	3.2679	0.0157	2.5603	0.03667	3.333	0.00987	3.1992
2	0.00614	3.114	0.01192	3.9879	0.0054	3.0917	0.00042	5.235	0.00272	3.7524	0.00031	4.9781
3	0.0005	3.6293	0.00126	3.2469	0.00038	3.8381	$9.6 \cdot 10^{-6}$	5.438	0.00005	5.6651	$8.3 \cdot 10^{-6}$	5.2331
4	0.00004	3.7407	0.0001	3.5831	0.00003	3.7617	$2.6 \cdot 10^{-7}$	5.2044	$1.3 \cdot 10^{-6}$	5.3824	$2.3 \cdot 10^{-7}$	5.1522
5	$2.5 \cdot 10^{-6}$	3.9087	$7.4 \cdot 10^{-6}$	3.8275	$1.9 \cdot 10^{-6}$	3.8892	$7.5 \cdot 10^{-9}$	5.1122	$3.6 \cdot 10^{-8}$	5.1611	$6.7 \cdot 10^{-9}$	5.1263

Table 3: The relative H^0 -errors with the estimated convergence rates (c.r.; the dyadic logarithm of the ratio of two consecutive relative errors) obtained by approximating the function z , defined in (15), using L^2 norm minimization (see Example 8 and Fig. 8, first and second row).

restricted to the different domains, see Fig. 8 (second row). The resulting H^0 -errors (i.e. L^2 -errors) and convergence rates for the different level L of refinement are presented in Table 3. The numerical results indicate that the convergence rate is optimal with respect to the H^0 -norm, which is $\mathcal{O}(h^4)$ and $\mathcal{O}(h^5)$ for bicubic and biquartic cases, respectively. \diamond

4.3. Poisson's equation

We consider again a two-patch domain $\Omega = \Omega^{(1)} \cup \Omega^{(2)}$, and a set $\{w_i\}_{i \in I}$ for $I = \{1, 2, \dots, \dim V_{0,0h}\}$ of C^1 -smooth geometrically continuous isogeometric functions, which form a basis of a subspace $V_{0,0h} \subset H_0^1(\Omega)$. We consider the following problem for the unknown function u over the computational domain Ω ,

$$\begin{cases} \Delta u(\mathbf{x}) = f(\mathbf{x}) & \text{on } \Omega \\ u(\mathbf{x}) = 0 & \text{on } \partial\Omega \end{cases} \quad (16)$$

with $f \in H^0(\Omega)$. Using the weak formulation and applying isogeometric Galerkin projection (cf. [9]) leads to a system of linear equations

$$S\mathbf{c} = \mathbf{f}$$

for the unknown coefficients $\mathbf{c} = (c_i)_{i \in I}$, where the entries of the stiffness matrix $S = (s_{i,j})_{i,j \in I}$ and of the load vector $\mathbf{f} = (f_i)_{i \in I}$ are given by

$$s_{i,j} = \int_{\Omega} (\nabla w_i(\mathbf{x}))^T \nabla w_j(\mathbf{x}) d\mathbf{x} \quad \text{and} \quad f_i = \int_{\Omega} f(\mathbf{x}) w_i(\mathbf{x}) d\mathbf{x},$$

respectively. Using the isogeometric approach, we rewrite these integrals as

$$s_{i,j} = s_{i,j}^{(1)} + s_{i,j}^{(2)}, \quad s_{i,j}^{(\ell)} = \int_{[0,1]^2} (\nabla W_i^{(\ell)}(\boldsymbol{\xi}^{(\ell)}))^T N^{(\ell)}(\boldsymbol{\xi}^{(\ell)}) \nabla W_j^{(\ell)}(\boldsymbol{\xi}^{(\ell)}) d\boldsymbol{\xi}^{(\ell)}, \quad \ell = 1, 2,$$

and

$$f_i = f_i^{(1)} + f_i^{(2)}, \quad f_i^{(\ell)} = \int_{[0,1]^2} f(\mathbf{G}^{(\ell)}(\boldsymbol{\xi}^{(\ell)})) W_i^{(\ell)}(\boldsymbol{\xi}^{(\ell)}) |\det J^{(\ell)}(\boldsymbol{\xi}^{(\ell)})| d\boldsymbol{\xi}^{(\ell)}, \quad \ell = 1, 2,$$

with

$$N^{(\ell)}(\boldsymbol{\xi}^{(\ell)}) = \left(J^{(\ell)}(\boldsymbol{\xi}^{(\ell)}) \right)^{-T} \left(J^{(\ell)}(\boldsymbol{\xi}^{(\ell)}) \right)^{-1} |\det J^{(\ell)}(\boldsymbol{\xi}^{(\ell)})|, \quad \ell = 1, 2.$$

L	Domain (a)				Domain (b)				Domain (c)			
	$\frac{\ u-u_h\ _0}{\ u\ _0}$	c.r. $\ \cdot\ _0$	$\frac{\ u-u_h\ _1}{\ u\ _1}$	c.r. $\ \cdot\ _1$	$\frac{\ u-u_h\ _0}{\ u\ _0}$	c.r. $\ \cdot\ _0$	$\frac{\ u-u_h\ _1}{\ u\ _1}$	c.r. $\ \cdot\ _1$	$\frac{\ u-u_h\ _0}{\ u\ _0}$	c.r. $\ \cdot\ _0$	$\frac{\ u-u_h\ _1}{\ u\ _1}$	c.r. $\ \cdot\ _1$
	Bicubic											
0	0.76824	-	0.79715	-	0.85307	-	0.78634	-	0.77419	-	0.79388	-
1	0.0312	4.6219	0.06712	3.5701	0.15608	2.4504	0.21366	1.8798	0.08635	3.1645	0.16776	2.2425
2	0.00145	4.4272	0.00762	3.1382	0.0053	4.88	0.01752	3.6084	0.01184	2.867	0.03805	2.1406
3	0.00009	4.0313	0.00097	2.9709	0.00021	4.625	0.00177	3.3082	0.00055	4.4407	0.00402	3.2438
4	$5.7 \cdot 10^{-6}$	3.9702	0.00012	2.9675	0.00001	4.2529	0.00021	3.0843	0.00003	4.4278	0.00048	3.0505
5	$3.6 \cdot 10^{-7}$	3.9765	0.00002	2.981	$6.8 \cdot 10^{-7}$	4.0479	0.00003	3.014	$1.5 \cdot 10^{-6}$	4.0772	0.00006	2.9304
	Biquartic											
0	0.01303	-	0.0256	-	0.16407	-	0.20565	-	0.06356	-	0.10765	-
1	0.00059	4.4648	0.00207	3.6269	0.0064	4.6792	0.01542	3.7376	0.01069	2.5717	0.03546	1.6022
2	0.00002	4.8915	0.00013	3.9454	0.0002	5.0164	0.00094	4.0393	0.00055	4.2792	0.00341	3.3765
3	$5.6 \cdot 10^{-7}$	5.1539	$7.8 \cdot 10^{-6}$	4.1024	$5.3 \cdot 10^{-6}$	5.2141	0.00005	4.2045	0.00002	4.9272	0.00023	3.9074
4	$1.4 \cdot 10^{-8}$	5.3021	$4.3 \cdot 10^{-7}$	4.18	$1.3 \cdot 10^{-7}$	5.3376	$2.6 \cdot 10^{-6}$	4.2651	$5 \cdot 10^{-7}$	5.1786	0.00001	4.0898
5	$3.5 \cdot 10^{-10}$	5.3383	$2.4 \cdot 10^{-8}$	4.1744	$3.2 \cdot 10^{-9}$	5.3586	$1.4 \cdot 10^{-7}$	4.2482	$1.3 \cdot 10^{-8}$	5.2902	$7.5 \cdot 10^{-7}$	4.1526

Table 4: The relative H^i -errors, $i = 0, 1$, with the corresponding estimated convergence rates (c.r.: the dyadic logarithm of the ratio of two consecutive relative errors) obtained by solving Poisson's equations for different exact solutions u , for the domains (a)-(c) (see Example 9 and Fig. 8, first and third row).

Example 9. We consider again the three computational domains, which are shown in Fig. 8 (first row). For each of the domains (a)-(c) we consider a different right side function f of Poisson's equation (16), which are obtained by differentiating

$$u_a(x_1, x_2) = 10^{-\frac{5}{2}} x_2 \left(\frac{1}{12} x_1 + x_2 \right) (4x_1 + x_2 - 14) \left(\frac{1}{3} x_1 + x_2 - 3 \right) \left(\frac{1}{8} x_1 - x_2 + 3 \right) \left(\frac{9}{4} x_1 + x_2 + \frac{13}{2} \right),$$

$$u_b(x_1, x_2) = \frac{1}{20\sqrt{10}} \left(\frac{18}{25} x_1 - x_2 \right) (x_1 + x_2) \left(3 + \frac{21}{20} x_1 - x_2 \right) \left(3 - \frac{25}{48} x_1 - x_2 \right) \left(\frac{19}{10} + \frac{21}{50} x_1 + x_2 \right) \left(\frac{290}{93} - \frac{110}{93} x_1 + x_2 \right),$$

and

$$u_c(x_1, x_2) = \frac{1}{100\sqrt{2}} \left(2 \left(\frac{128327}{48672} + x_1 \right) + \left(x_2 - \frac{185}{156} \right)^2 \right) \left(2 \left(\frac{215}{72} - x_1 \right) + \left(x_2 - \frac{11}{6} \right)^2 \right) \left(\frac{1}{9} x_1 + x_2 \right) \left(\frac{3}{10} x_1 - x_2 \right) \left(3 + \frac{1}{7} x_1 - x_2 \right) \left(3 - \frac{1}{3} x_1 - x_2 \right),$$

respectively. The three functions satisfy the boundary conditions $u = 0$ on $\partial\Omega$, and are visualized in Fig. 8 (third row). The resulting H^i -errors, $i = 0, 1$, with the corresponding convergence rates are presented in Table 4. The numerical results indicate convergence rates of $\mathcal{O}(h^{4-i})$ and $\mathcal{O}(h^{5-i})$ in the H^i -norms, $i = 0, 1$, for the bicubic and the biquartic case, respectively. \diamond

4.4. Biharmonic equation

Higher order smoothness of isogeometric elements is particularly advantageous for solving high order partial differential equations. An example of such an equation is (the weak formulation of) the biharmonic equation, where C^1 -smoothness of isogeometric functions is an advantage, since test functions from the space $H^2(\Omega)$ are required (cf. [8, 22]).

Let $\{w_i\}_{i \in I}$ for $I = \{1, 2, \dots, \dim V_{1,0h}\}$ be a set of C^1 -smooth geometrically continuous isogeometric functions, which form a basis of a subspace $V_{1,0h}$ of $H_0^2(\Omega)$, where $\Omega = \Omega^{(1)} \cup$

$\Omega^{(2)}$ is a two-patch domain. As a model problem we consider the first biharmonic boundary value problem for the unknown function u over the computational domain Ω ,

$$\begin{cases} \Delta^2 u(\mathbf{x}) = f(\mathbf{x}) & \text{on } \Omega \\ u(\mathbf{x}) = \frac{\partial u}{\partial \mathbf{n}}(\mathbf{x}) = 0 & \text{on } \partial\Omega \end{cases}, \quad (17)$$

with $f \in H^0(\Omega)$. Using the weak formulation, we compute $u \in H_0^2(\Omega)$ such that

$$\int_{\Omega} \Delta u(\mathbf{x}) \Delta v(\mathbf{x}) d\mathbf{x} = \int_{\Omega} f(\mathbf{x}) v(\mathbf{x}) d\mathbf{x}$$

for all $v \in H_0^2(\Omega)$ (see [22]). Using the Galerkin projection we find $v_h \in V_{1,0h}$ by solving the system of equations

$$\int_{\Omega} \Delta u_h(\mathbf{x}) \Delta v_h(\mathbf{x}) d\mathbf{x} = \int_{\Omega} f(\mathbf{x}) v_h(\mathbf{x}) d\mathbf{x}$$

for all $v_h \in V_{1,0h}$, which leads to a system of linear equations. More precisely, we are solving the linear system $S\mathbf{c} = \mathbf{f}$, for the coefficients of

$$u_h(\mathbf{x}) = \sum_{i \in I} c_i w_i(\mathbf{x}),$$

where

$$s_{i,j} = \int_{\Omega} \Delta w_i(\mathbf{x}) \Delta w_j(\mathbf{x}) d\mathbf{x} \quad \text{and} \quad f_i = \int_{\Omega} f(\mathbf{x}) w_i(\mathbf{x}) d\mathbf{x},$$

respectively. After some computations we arrive at the following formulas for the elements of the stiffness matrix and the load vector for the two-patch isogeometric case:

$$s_{i,j} = s_{i,j}^{(1)} + s_{i,j}^{(2)}, \quad s_{i,j}^{(\ell)} = \int_{[0,1]^2} \text{tr} \left(\widetilde{M}_i^{(\ell)}(\boldsymbol{\xi}^{(\ell)}) \right) \text{tr} \left(\widetilde{M}_j^{(\ell)}(\boldsymbol{\xi}^{(\ell)}) \right) \frac{1}{|\det J^{(\ell)}(\boldsymbol{\xi}^{(\ell)})|} d\boldsymbol{\xi}^{(\ell)}, \quad \ell = 1, 2,$$

and

$$f_i = f_i^{(1)} + f_i^{(2)}, \quad f_i^{(\ell)} = \int_{[0,1]^2} f(\mathbf{G}^{(\ell)}(\boldsymbol{\xi}^{(\ell)})) W_i^{(\ell)}(\boldsymbol{\xi}^{(\ell)}) |\det J^{(\ell)}(\boldsymbol{\xi}^{(\ell)})| d\boldsymbol{\xi}^{(\ell)}, \quad \ell = 1, 2,$$

with

$$\widetilde{M}_i^{(\ell)}(\boldsymbol{\xi}^{(\ell)}) = \left(J^{(\ell)}(\boldsymbol{\xi}^{(\ell)}) \right)^{-T} M_i^{(\ell)}(\boldsymbol{\xi}^{(\ell)}) \left(J^{(\ell)}(\boldsymbol{\xi}^{(\ell)}) \right)^{-1},$$

where $M_i^{(\ell)} = \left(m_{i;r,s}^{(\ell)} \right)_{r,s=1,2}$ is given by

$$m_{i;r,s}^{(\ell)} = \left(\frac{\partial^2 \mathbf{F}_i^{(\ell)}}{\partial \xi_r^{(\ell)} \partial \xi_s^{(\ell)}}(\boldsymbol{\xi}^{(\ell)}) \right)^T \cdot \left(\frac{\partial \mathbf{F}_i^{(\ell)}}{\partial \xi_1^{(\ell)}}(\boldsymbol{\xi}^{(\ell)}) \times \frac{\partial \mathbf{F}_i^{(\ell)}}{\partial \xi_2^{(\ell)}}(\boldsymbol{\xi}^{(\ell)}) \right).$$

L	Bicubic						Biquartic					
	$\frac{\ u-u_h\ _0}{\ u\ _0}$	c.r. $\ \cdot\ _0$	$\frac{\ u-u_h\ _1}{\ u\ _1}$	c.r. $\ \cdot\ _1$	$\frac{\ u-u_h\ _2}{\ u\ _2}$	c.r. $\ \cdot\ _2$	$\frac{\ u-u_h\ _0}{\ u\ _0}$	c.r. $\ \cdot\ _0$	$\frac{\ u-u_h\ _1}{\ u\ _1}$	c.r. $\ \cdot\ _1$	$\frac{\ u-u_h\ _2}{\ u\ _2}$	c.r. $\ \cdot\ _2$
	Domain (a)											
1	-	-	-	-	-	-	0.03487	-	0.0825	-	0.21691	-
2	0.0854	-	0.10026	-	0.19868	-	0.01122	1.6367	0.01529	2.4316	0.04748	2.1916
3	0.01023	3.0619	0.01322	2.9231	0.04907	2.0175	0.00068	4.0498	0.00118	3.6939	0.0077	2.6253
4	0.00099	3.3717	0.00147	3.1638	0.01207	2.0237	0.00003	4.6554	0.00006	4.2169	0.00095	3.0169
5	0.00007	3.9088	0.00013	3.5344	0.00286	2.0758	$8.8 \cdot 10^{-7}$	4.9244	$3.2 \cdot 10^{-6}$	4.3237	0.00011	3.0704
	Domain (b)											
1	-	-	-	-	-	-	0.28053	-	0.36533	-	0.45296	-
2	0.26249	-	0.35642	-	0.46964	-	0.0067	5.3871	0.0182	4.327	0.05738	2.9808
3	0.00751	5.1264	0.01511	4.5602	0.07582	2.6309	0.00059	3.6641	0.00235	2.9509	0.01407	2.0271
4	0.0007	3.4276	0.00252	2.5817	0.0214	1.825	0.00002	4.9899	0.00015	3.935	0.00187	2.9112
5	0.00004	4.0957	0.00026	3.3062	0.00514	2.0572	$3.7 \cdot 10^{-7}$	5.4819	$7.9 \cdot 10^{-6}$	4.2917	0.0002	3.206
	Domain (c)											
1	-	-	-	-	-	-	0.15127	-	0.19195	-	0.34591	-
2	0.23492	-	0.26927	-	0.39737	-	0.00435	5.12	0.01153	4.0569	0.06199	2.4803
3	0.0037	5.9883	0.00827	5.0256	0.06516	2.6084	0.00141	1.6242	0.00273	2.0813	0.01605	1.9491
4	0.00149	1.3077	0.00266	1.637	0.01976	1.7218	0.00008	4.076	0.00022	3.6083	0.00284	2.499
5	0.00014	3.4688	0.0003	3.1319	0.00491	2.0072	$3.2 \cdot 10^{-6}$	4.7036	0.00001	4.1635	0.00036	2.9718

Table 5: The relative H^i -errors, $i = 0, 1, 2$, with the corresponding estimated convergence rates (c.r.; the dyadic logarithm of the ratio of two consecutive relative errors) obtained by solving the biharmonic equations for different exact solutions \tilde{u} , for the domains (a)-(c) (see Example 10 and Fig. 8, first and fourth row).

Example 10. We numerically solve the biharmonic equation (17) over the same three computational domains Ω with the same associated initial geometry mappings $\mathbf{G}^{(1)}$ and $\mathbf{G}^{(2)}$ as in Example 8 and 9 (see Fig. 8, first row). We use the nested spaces $V_{1,0h} \subset H_0^2(\Omega)$ of C^1 -smooth geometrically continuous isogeometric functions for degree $d = 3, 4$, where the number of resulting functions (for each level L) are presented in Table 2. Note, that for the bicubic and the biquartic case, there do not exist non-trivial geometrically continuous isogeometric functions for low levels L , due to the boundary conditions. Therefore, the coarsest level starts with $L = 2$ and $L = 1$ for $d = 3$ and $d = 4$, respectively.

The right-hand side functions f of the biharmonic equation (17) for the domains (a)-(c) are obtained by differentiating the functions $\tilde{u} = u^2$, where u are the corresponding functions from Example 9. These functions fulfill the boundary conditions $\tilde{u} = \frac{\partial \tilde{u}}{\partial \mathbf{n}} = 0$ on $\partial\Omega$, and are visualized in Fig. 8 (fourth row). The resulting H^i -errors, $i = 0, 1, 2$, with the corresponding convergence rates are presented in Table 5. The numerical results indicate a convergence rate of $\mathcal{O}(h^2)$ and $\mathcal{O}(h^3)$ in the H^2 -norm for the bicubic and the biquartic case, respectively. \diamond

Example 11. Table 6 reports the condition numbers κ and the estimated growth rate for the three matrices considered in the numerical experiments with domain (a) in Fig. 8 and $d = 4$. Diagonal scaling was applied to all matrices, cf. [6]. These numerical results indicate that using geometric continuity does not have much impact on the growth rate of the condition numbers. \diamond

L	L^2 approximation		Poisson's equation		Biharmonic equation	
	$\kappa(D^{-\frac{1}{2}}KD^{-\frac{1}{2}})$	rate	$\kappa(D^{-\frac{1}{2}}SD^{-\frac{1}{2}})$	rate	$\kappa(D^{-\frac{1}{2}}SD^{-\frac{1}{2}})$	rate
1	4770.34	-	127.35	-	10.85	-
2	5351.16	0.1658	184.43	0.5343	115.2	3.4085
3	5307.29	-0.0119	210.51	0.1908	2041.25	4.1472
4	5254.07	-0.0145	224.08	0.0901	35038.22	4.1014
5	5248.63	-0.0014	723.73	1.6914	587462.26	4.0675

Table 6: Condition numbers κ with the estimate growth rate (the dyadic logarithmic of the ratio of two consecutive condition numbers), see Example 11 for details.

5. Conclusion

We discussed C^s -smooth geometrically continuous isogeometric functions defined on multi-patch domains $\Omega \subset \mathbb{R}^2$. Their construction is based on the observation that the geometric smoothness of the graph of such a function is equivalent to the smoothness of the function over Ω . We also sketched a procedure to construct a basis for the space of C^s -smooth geometrically continuous isogeometric functions. Special attention was paid to the case of bilinearly parameterized two-patch geometries, where we were able to present the construction in more detail.

The potential of the resulting geometrically continuous isogeometric functions has been demonstrated by several examples, including L^2 approximation, Poisson's equation and the biharmonic equation. For these examples, we considered different two patch-domains Ω consisting of two quadrilateral patches, for which we generated geometrically continuous isogeometric functions of order 1 and degree $d = 3, 4$. For all three different applications, the numerical results indicated optimal convergence rates.

This is different from the experiments reported in [16], where a reduction of the order of convergence for geometrically continuous discretizations has been observed. A possible explanation is the fact that the effect of geometric continuity in those experiments was concentrated at an extraordinary vertex, while we spread it out along the entire interface between two patches. In fact, many constructions for geometrically continuous surfaces in geometric modeling aim at limiting the effect of geometric continuity to the vicinity of extraordinary vertices [18], as it is then possible to use standard constructions everywhere except at very few places. However, our experiments seem to indicate that spreading out the effect of geometric continuity is more appropriate for applications in isogeometric analysis, in order to maintain the approximation power. Moreover, the latter approach makes it also simpler to obtain nested spaces by h -refinement.

The detailed construction of the basis functions presented in this paper is restricted to two-patch domains. In order to overcome this limitation, we are currently working on using our general framework to generate C^1 -smooth geometrically continuous isogeometric functions for multi-patch domains with extraordinary vertices. A detailed investigation of the structure of the resulting spaces of geometrically continuous isogeometric functions is of interest, too. On the one hand we could generate basis functions with a small support, if feasible. On the other hand we aim at finding explicit formulas, depending on the initial geometry, for the coefficients of the isogeometric functions. Related results have recently become available as a technical report [4], especially focusing on higher degrees and special

configurations.

Another possible topic of future work is a theoretical investigation of the approximation power of geometrically continuous isogeometric functions. For bilinearly parameterized two-patch domains, the space of these functions contains the spline space of the C^1 -smooth spline functions of degree d on the quadrangular partition of the domain determined by the knot lines in the parameter domains. There exist dimension results for this type of spline spaces [15] but the approximation power has not yet been investigated.

Finally, the extension of the concept of geometrically continuous isogeometric functions to three-dimensional multi-patch domains should be considered.

Acknowledgments. Supported by the Austrian Research Fund (FWF) through Grant NFN (National Research Network) S117 “Geometry +Simulation”.

Appendix A. Basis functions of the second kind for $d = 4$

We provide simple explicit formulas for the Bézier coefficients of the basis functions of the second kind in the generic case for $d = 4$ and bilinearly parameterized two-patch domains Ω (see Section 3.3). These basis functions have been categorized into 4 types, see Fig. 6, according to the number of spline segments in their support. The values of the Bézier coefficients are given with respect to the corresponding local geometry specified in Fig. 5, where the left and right geometry applies to types A, L, U and B, respectively. All coefficients not specified in the equations below take the value zero.

- Type A.1:

$$\hat{a}_6 = 1, \hat{a}_8 = \frac{\hat{p}_2}{\hat{p}_0}, \hat{a}_9 = 1 + \frac{3\hat{p}_1}{4\hat{p}_0}, \hat{a}_{11} = \frac{4\hat{p}_2 + 3\hat{p}_3}{4\hat{p}_0}, \hat{a}_{12} = \frac{\hat{p}_0 + \hat{p}_1}{2\hat{p}_0}, \hat{a}_{14} = \frac{\hat{p}_2 + \hat{p}_3}{2\hat{p}_0}, \hat{a}_{15} = \frac{\hat{p}_1}{4\hat{p}_0},$$

$$\hat{a}_{17} = \frac{\hat{p}_3}{4\hat{p}_0}.$$

- Type A.2:

$$\hat{a}_8 = \frac{-\hat{p}_2\hat{q}_0 + \hat{p}_0\hat{q}_2}{2\hat{p}_0}, \hat{a}_9 = \frac{-3\hat{p}_1\hat{p}_3\hat{q}_0 + \hat{p}_0\hat{p}_3(2-\hat{q}_0+3\hat{q}_1) + \hat{p}_0^2(-2+\hat{q}_3)}{8\hat{p}_0\hat{p}_3}, \hat{a}_{10} = 1,$$

$$\hat{a}_{11} = \frac{-\hat{p}_3(4\hat{p}_2+3\hat{p}_3)\hat{q}_0 + \hat{p}_0(\hat{p}_2(-2+\hat{q}_3) + \hat{p}_3(2+3\hat{q}_2+3\hat{q}_3))}{8\hat{p}_0\hat{p}_3},$$

$$\hat{a}_{12} = \frac{-\hat{p}_1\hat{p}_3\hat{q}_0 + \hat{p}_0(-\hat{p}_3(-4+\hat{q}_0) + \hat{p}_1(-2+\hat{q}_3)) + \hat{p}_0^2(-2+\hat{q}_3)}{4\hat{p}_0\hat{p}_3},$$

$$\hat{a}_{13} = 1, \hat{a}_{14} = \frac{-\hat{p}_3(\hat{p}_2 + \hat{p}_3)\hat{q}_0 + \hat{p}_0(\hat{p}_2(-2+\hat{q}_3) + \hat{p}_3(2+\hat{q}_3))}{4\hat{p}_0\hat{p}_3},$$

$$\hat{a}_{15} = \frac{-\hat{p}_1\hat{p}_3\hat{q}_0 + \hat{p}_0(\hat{p}_3(14-3\hat{q}_0-3\hat{q}_1) + 4\hat{p}_1(-2+\hat{q}_3)) + 3\hat{p}_0^2(-2+\hat{q}_3)}{8\hat{p}_0\hat{p}_3},$$

$$\hat{a}_{16} = 1, \hat{a}_{17} = \frac{-\hat{p}_3^2\hat{q}_0 + \hat{p}_0(3\hat{p}_2(-2+\hat{q}_3) + \hat{p}_3(6-3\hat{q}_2+\hat{q}_3))}{8\hat{p}_0\hat{p}_3}, \hat{a}_{18} = \frac{-\hat{p}_3(-2+\hat{q}_1) + \hat{p}_1(-2+\hat{q}_3)}{2\hat{p}_3}.$$

- Type A.3:

$$\hat{a}_9 = \frac{\hat{p}_0}{4\hat{p}_3}, \hat{a}_{11} = \frac{\hat{p}_2}{4\hat{p}_3}, \hat{a}_{12} = \frac{\hat{p}_0 + \hat{p}_1}{2\hat{p}_3}, \hat{a}_{14} = \frac{\hat{p}_2 + \hat{p}_3}{2\hat{p}_3}, \hat{a}_{15} = \frac{3\hat{p}_0 + 4\hat{p}_1}{4\hat{p}_3}, \hat{a}_{17} = 1 + \frac{3\hat{p}_2}{4\hat{p}_3}, \hat{a}_{18} = \frac{\hat{p}_1}{\hat{p}_3},$$

$$\hat{a}_{20} = 1.$$

- Type B:

$$\begin{aligned}
\tilde{a}_{11} &= \frac{-\tilde{p}_2\tilde{q}_0+\tilde{p}_0\tilde{q}_2}{16\tilde{p}_0}, \tilde{a}_{12} = \frac{-\tilde{p}_1\tilde{q}_0+\tilde{p}_0\tilde{q}_1}{12\tilde{p}_0}, \tilde{a}_{13} = \frac{1}{4}, \tilde{a}_{14} = \frac{-2\tilde{p}_2\tilde{q}_0-\tilde{p}_3\tilde{q}_0+\tilde{p}_0(2\tilde{q}_2+\tilde{q}_3)}{12\tilde{p}_0}, \\
\tilde{a}_{15} &= \frac{-\tilde{p}_1\tilde{q}_0+\tilde{p}_0\tilde{q}_1}{6\tilde{p}_0}, \tilde{a}_{16} = \frac{1}{2}, \tilde{a}_{17} = \frac{-13\tilde{p}_2\tilde{q}_0-8\tilde{p}_3\tilde{q}_0+13\tilde{p}_0\tilde{q}_2+8\tilde{p}_0\tilde{q}_3}{48\tilde{p}_0}, \\
\tilde{a}_{18} &= \frac{-2\tilde{p}_1\tilde{p}_3\tilde{q}_0+\tilde{p}_0(\tilde{p}_3(9-2\tilde{q}_0+\tilde{q}_1)+\tilde{p}_1(-3+\tilde{q}_3))+2\tilde{p}_0^2(-3+\tilde{q}_3)}{12\tilde{p}_0\tilde{p}_3}, \tilde{a}_{19} = 1, \\
\tilde{a}_{20} &= \frac{-\tilde{p}_3(\tilde{p}_2+2\tilde{p}_3)\tilde{q}_0+\tilde{p}_0(2\tilde{p}_2(-3+\tilde{q}_3)+\tilde{p}_3(6-\tilde{q}_2+2\tilde{q}_3))}{12\tilde{p}_0\tilde{p}_3}, \\
\tilde{a}_{21} &= \frac{\tilde{p}_3(63-8\tilde{q}_0-13\tilde{q}_1)+8\tilde{p}_0(-3+\tilde{q}_3)+13\tilde{p}_1(-3+\tilde{q}_3)}{48\tilde{p}_3}, \tilde{a}_{22} = \frac{1}{2}, \\
\tilde{a}_{23} &= \frac{-\tilde{p}_3(-3+\tilde{q}_2)+\tilde{p}_2(-3+\tilde{q}_3)}{6\tilde{p}_3}, \tilde{a}_{24} = \frac{-\tilde{p}_3(-9+\tilde{q}_0+2\tilde{q}_1)+\tilde{p}_0(-3+\tilde{q}_3)+2\tilde{p}_1(-3+\tilde{q}_3)}{12\tilde{p}_3}, \tilde{a}_{25} = \frac{1}{4}, \\
\tilde{a}_{26} &= \frac{-\tilde{p}_3(-3+\tilde{q}_2)+\tilde{p}_2(-3+\tilde{q}_3)}{12\tilde{p}_3}, \tilde{a}_{27} = \frac{-\tilde{p}_3(-3+\tilde{q}_1)+\tilde{p}_1(-3+\tilde{q}_3)}{16\tilde{p}_3}.
\end{aligned}$$

- Type L.1:

$$\begin{aligned}
\hat{a}_0 &= \frac{-(\hat{p}_2+\hat{p}_3)(-1+\hat{q}_0)+\hat{p}_0(-2+\hat{q}_2+\hat{q}_3)}{\hat{p}_2+\hat{p}_3}, \hat{a}_1 = 1, \hat{a}_2 = \frac{\hat{p}_3-\hat{p}_3\hat{q}_2+\hat{p}_2(-1+\hat{q}_3)}{\hat{p}_2+\hat{p}_3}, \\
\hat{a}_3 &= \frac{-(\hat{p}_2+\hat{p}_3)(-2+\hat{q}_0+\hat{q}_1)+\hat{p}_0(-2+\hat{q}_2+\hat{q}_3)+\hat{p}_1(-2+\hat{q}_2+\hat{q}_3)}{8(\hat{p}_2+\hat{p}_3)}.
\end{aligned}$$

- Type L.2:

$$\hat{a}_1 = 1, \hat{a}_2 = \frac{\hat{p}_0+\hat{p}_2(-1+\hat{q}_0)-\hat{p}_0\hat{q}_2}{\hat{p}_0}, \hat{a}_3 = \frac{\hat{p}_0+\hat{p}_1(-1+\hat{q}_0)-\hat{p}_0\hat{q}_1}{8\hat{p}_0}, \hat{a}_5 = \frac{(\hat{p}_2+\hat{p}_3)(-1+\hat{q}_0)-\hat{p}_0(-2+\hat{q}_2+\hat{q}_3)}{8\hat{p}_0}.$$

- Type L.3:

$$\begin{aligned}
\hat{a}_2 &= \frac{-\hat{p}_2\hat{q}_0+\hat{p}_0\hat{q}_2}{\hat{p}_0}, \hat{a}_3 = -\frac{\hat{p}_1(\hat{p}_2+\hat{p}_3)\hat{q}_0+\hat{p}_0(\hat{p}_2+\hat{p}_3)(-6+6\hat{q}_0-\hat{q}_1)-6\hat{p}_0^2(-2+\hat{q}_2+\hat{q}_3)}{8\hat{p}_0(\hat{p}_2+\hat{p}_3)}, \hat{a}_4 = 1, \\
\hat{a}_5 &= \frac{-(\hat{p}_2+\hat{p}_3)^2\hat{q}_0+\hat{p}_0(\hat{p}_3(6-5\hat{q}_2+\hat{q}_3)+\hat{p}_2(-6+\hat{q}_2+7\hat{q}_3))}{8\hat{p}_0(\hat{p}_2+\hat{p}_3)}, \\
\hat{a}_6 &= \frac{-(\hat{p}_2+\hat{p}_3)(-2+\hat{q}_0+\hat{q}_1)+\hat{p}_0(-2+\hat{q}_2+\hat{q}_3)+\hat{p}_1(-2+\hat{q}_2+\hat{q}_3)}{4(\hat{p}_2+\hat{p}_3)}.
\end{aligned}$$

- Type L.4:

$$\hat{a}_3 = 1, \hat{a}_5 = \frac{\hat{p}_2}{\hat{p}_0}, \hat{a}_6 = \frac{\hat{p}_0+\hat{p}_1}{3\hat{p}_0}, \hat{a}_8 = \frac{\hat{p}_2+\hat{p}_3}{3\hat{p}_0}.$$

- Type L.5:

$$\begin{aligned}
\hat{a}_5 &= \frac{3(-\hat{p}_2\hat{q}_0+\hat{p}_0\hat{q}_2)}{4\hat{p}_0}, \hat{a}_6 = \frac{-\hat{p}_1\hat{p}_3\hat{q}_0+\hat{p}_0\hat{p}_3(2-\hat{q}_0+\hat{q}_1)+\hat{p}_0^2(-2+\hat{q}_3)}{4\hat{p}_0\hat{p}_3}, \hat{a}_7 = 1, \\
\hat{a}_8 &= \frac{-\hat{p}_3(\hat{p}_2+\hat{p}_3)\hat{q}_0+\hat{p}_0(\hat{p}_2(-2+\hat{q}_3)+\hat{p}_3(2+\hat{q}_3))}{4\hat{p}_0\hat{p}_3}, \hat{a}_9 = \frac{\hat{p}_3(14-4\hat{q}_0-3\hat{q}_1)+4\hat{p}_0(-2+\hat{q}_3)+3\hat{p}_1(-2+\hat{q}_3)}{16\hat{p}_3}, \\
\hat{a}_{10} &= \frac{1}{2}, \hat{a}_{11} = \frac{-\hat{p}_3(-2+\hat{q}_2)+\hat{p}_2(-2+\hat{q}_3)}{4\hat{p}_3}, \hat{a}_{12} = \frac{-\hat{p}_3(-4+\hat{q}_0+\hat{q}_1)+\hat{p}_0(-2+\hat{q}_3)+\hat{p}_1(-2+\hat{q}_3)}{8\hat{p}_3}, \hat{a}_{13} = \frac{1}{4}, \\
\hat{a}_{14} &= \frac{-\hat{p}_3(-2+\hat{q}_2)+\hat{p}_2(-2+\hat{q}_3)}{8\hat{p}_3}, \hat{a}_{15} = \frac{-\hat{p}_3(-2+\hat{q}_1)+\hat{p}_1(-2+\hat{q}_3)}{16\hat{p}_3}.
\end{aligned}$$

- Type U.1:

$$\begin{aligned}
\hat{a}_{23} &= \frac{-(\hat{p}_2+\hat{p}_3)(-2+\hat{q}_0+\hat{q}_1)+\hat{p}_0(-2+\hat{q}_2+\hat{q}_3)+\hat{p}_1(-2+\hat{q}_2+\hat{q}_3)}{8(\hat{p}_0+\hat{p}_1)}, \hat{a}_{24} = \frac{\hat{p}_1-\hat{p}_1\hat{q}_0+\hat{p}_0(-1+\hat{q}_1)}{\hat{p}_0+\hat{p}_1}, \\
\hat{a}_{25} &= 1, \hat{a}_{26} = \frac{-\hat{p}_3(-2+\hat{q}_0+\hat{q}_1)+\hat{p}_0(-1+\hat{q}_3)+\hat{p}_1(-1+\hat{q}_3)}{\hat{p}_0+\hat{p}_1}.
\end{aligned}$$

- Type U.2:

$$\hat{a}_{21} = \frac{\hat{p}_0 + \hat{p}_1 + \hat{p}_3(-2 + \hat{q}_0 + \hat{q}_1) - \hat{p}_0 \hat{q}_3 - \hat{p}_1 \hat{q}_3}{8\hat{p}_3}, \hat{a}_{23} = \frac{\hat{p}_2 + \hat{p}_3(-1 + \hat{q}_2) - \hat{p}_2 \hat{q}_3}{8\hat{p}_3}, \hat{a}_{24} = \frac{\hat{p}_1 + \hat{p}_3(-1 + \hat{q}_1) - \hat{p}_1 \hat{q}_3}{\hat{p}_3},$$

$$\hat{a}_{25} = 1.$$

- Type U.3:

$$\hat{a}_{20} = \frac{-(\hat{p}_2 + \hat{p}_3)(-2 + \hat{q}_0 + \hat{q}_1) + \hat{p}_0(-2 + \hat{q}_2 + \hat{q}_3) + \hat{p}_1(-2 + \hat{q}_2 + \hat{q}_3)}{4(\hat{p}_0 + \hat{p}_1)},$$

$$\hat{a}_{21} = \frac{\hat{p}_1(-\hat{p}_3(-10 + 7\hat{q}_0 + \hat{q}_1) + \hat{p}_1(-2 + \hat{q}_3)) + \hat{p}_0(-\hat{p}_3(2 + \hat{q}_0 - 5\hat{q}_1) + 2\hat{p}_1(-2 + \hat{q}_3)) + \hat{p}_0^2(-2 + \hat{q}_3)}{8(\hat{p}_0 + \hat{p}_1)\hat{p}_3}, \hat{a}_{22} = 1,$$

$$\hat{a}_{23} = \frac{-6\hat{p}_3^2(-2 + \hat{q}_0 + \hat{q}_1) + \hat{p}_0(-\hat{p}_3(4 + \hat{q}_2 - 6\hat{q}_3) + \hat{p}_2(-2 + \hat{q}_3)) + \hat{p}_1(-\hat{p}_3(4 + \hat{q}_2 - 6\hat{q}_3) + \hat{p}_2(-2 + \hat{q}_3))}{8(\hat{p}_0 + \hat{p}_1)\hat{p}_3},$$

$$\hat{a}_{24} = \frac{-\hat{p}_3(-2 + \hat{q}_1) + \hat{p}_1(-2 + \hat{q}_3)}{\hat{p}_3}.$$

- Type U.4:

$$\hat{a}_{18} = \frac{\hat{p}_0 + \hat{p}_1}{3\hat{p}_3}, \hat{a}_{20} = \frac{\hat{p}_2 + \hat{p}_3}{3\hat{p}_3}, \hat{a}_{21} = \frac{\hat{p}_1}{\hat{p}_3}, \hat{a}_{23} = 1.$$

- Type U.5:

$$\hat{a}_{11} = \frac{-\hat{p}_2 \hat{q}_0 + \hat{p}_0 \hat{q}_2}{16\hat{p}_0}, \hat{a}_{12} = \frac{-\hat{p}_1 \hat{q}_0 + \hat{p}_0 \hat{q}_1}{8\hat{p}_0}, \hat{a}_{13} = \frac{1}{4}, \hat{a}_{14} = -\frac{\hat{p}_2 \hat{q}_0 + \hat{p}_3 \hat{q}_0 - \hat{p}_0(\hat{q}_2 + \hat{q}_3)}{8\hat{p}_0},$$

$$\hat{a}_{15} = \frac{-\hat{p}_1 \hat{q}_0 + \hat{p}_0 \hat{q}_1}{4\hat{p}_0}, \hat{a}_{16} = \frac{1}{2}, \hat{a}_{17} = \frac{-3\hat{p}_2 \hat{q}_0 - 4\hat{p}_3 \hat{q}_0 + 3\hat{p}_0 \hat{q}_2 + 4\hat{p}_0 \hat{q}_3}{16\hat{p}_0},$$

$$\hat{a}_{18} = \frac{-\hat{p}_1 \hat{p}_3 \hat{q}_0 + \hat{p}_0(-\hat{p}_3(-4 + \hat{q}_0) + \hat{p}_1(-2 + \hat{q}_3)) + \hat{p}_0^2(-2 + \hat{q}_3)}{4\hat{p}_0 \hat{p}_3}, \hat{a}_{19} = 1,$$

$$\hat{a}_{20} = \frac{-\hat{p}_3^2 \hat{q}_0 + \hat{p}_0(\hat{p}_2(-2 + \hat{q}_3) + \hat{p}_3(2 - \hat{q}_2 + \hat{q}_3))}{4\hat{p}_0 \hat{p}_3}, \hat{a}_{21} = \frac{3(-\hat{p}_3(-2 + \hat{q}_1) + \hat{p}_1(-2 + \hat{q}_3))}{4\hat{p}_3}.$$

References

- [1] Y. Bazilevs, V. M. Calo, J. A. Cottrell, J. A. Evans, T. J. R. Hughes, S. Lipton, M. A. Scott, and T. W. Sederberg. Isogeometric analysis using T-splines. *Computer Methods in Applied Mechanics and Engineering*, 199(5–8):229 – 263, 2010.
- [2] L. Beirão da Veiga, A. Buffa, D. Cho, and G. Sangalli. IsoGeometric analysis using T-splines on two-patch geometries. *Computer Methods in Applied Mechanics and Engineering*, 200(21–22):1787 – 1803, 2011.
- [3] L. Beirão da Veiga, A. Buffa, G. Sangalli, and R. Vázquez. Mathematical analysis of variational isogeometric methods. *Acta Numerica*, 23:157–287, 5 2014.
- [4] M. Bercovier and T. Matskewich. Smooth Bézier surfaces over arbitrary quadrilateral meshes. Technical Report 1412.1125, arXiv.org, 2014.
- [5] K. Birner. C^1 -smooth geometrically continuous test functions on bilinearly parameterized multi-patch domains. Master’s thesis, Johannes Kepler University, Linz, 2015. in progress.
- [6] A. M. Bruaset. *A survey of preconditioned iterative methods*, volume 328 of *Pitman Research Notes in Mathematics Series*. Longman Scientific & Technical, Harlow, 1995.
- [7] D. Burkhart, B. Hamann, and G. Umlauf. Iso-geometric analysis based on Catmull-Clark solid subdivision. *Computer Graphics Forum*, 29(5):1575–1784, 2010.

- [8] P. G. Ciarlet. *The Finite Element Method for Elliptic Problems*. Society for Industrial and Applied Mathematics, 2002.
- [9] J. A. Cottrell, T.J.R. Hughes, and Y. Bazilevs. *Isogeometric Analysis: Toward Integration of CAD and FEA*. John Wiley & Sons, Chichester, England, 2009.
- [10] D. Groisser and J. Peters. Matched G^k -constructions always yield C^k -continuous isogeometric elements. *Computer Aided Geometric Design*, 2015. In Press.
- [11] J. Hoschek and D. Lasser. *Fundamentals of computer aided geometric design*. A K Peters Ltd., Wellesley, MA, 1993.
- [12] T. J. R. Hughes, J. A. Cottrell, and Y. Bazilevs. Isogeometric analysis: CAD, finite elements, NURBS, exact geometry and mesh refinement. *Comput. Methods Appl. Mech. Engrg.*, 194(39-41):4135–4195, 2005.
- [13] H.-J. Kim, Y.-D. Seo, and S.-K. Youn. Isogeometric analysis with trimming technique for problems of arbitrary complex topology. *Computer Methods in Applied Mechanics and Engineering*, 199(45–48):2796 – 2812, 2010.
- [14] S. Kleiss, C. Pechstein, B. Jüttler, and S. Tomar. IETI – isogeometric tearing and interconnecting. *Computer Methods in Applied Mechanics and Engineering*, 247-248:201–215, 2012.
- [15] C. Manni. On the dimension of bivariate spline spaces on generalized quasi-cross-cut partitions. *J. Approx. Theory*, 69(2):141–155, 1992.
- [16] T. Nguyen, K. Karčiauskas, and J. Peters. A comparative study of several classical, discrete differential and isogeometric methods for solving poisson’s equation on the disk. *Axioms*, 3(2):280–299, 2014.
- [17] V.P. Nguyen, P. Kerfriden, M. Brino, S.P.A. Bordas, and E. Bonisoli. Nitsche’s method for two and three dimensional NURBS patch coupling. *Comput. Mech.*, 53(6):1163–1182, 2014.
- [18] J. Peters. Geometric continuity. In *Handbook of computer aided geometric design*, pages 193–227. North-Holland, Amsterdam, 2002.
- [19] J. Peters and U. Reif. *Subdivision surfaces*, volume 3 of *Geometry and Computing*. Springer-Verlag, Berlin, 2008.
- [20] L. Piegl and W. Tiller. *The NURBS Book*. Springer, 1997.
- [21] M. Ruess, D. Schillinger, A. I. Özcan, and E. Rank. Weak coupling for isogeometric analysis of non-matching and trimmed multi-patch geometries. *Computer Methods in Applied Mechanics and Engineering*, 269:46 – 71, 2014.
- [22] Sandro Salsa. *Partial differential equations in action: From modelling to theory*. Universitext. Springer-Verlag Italia, Milan, 2008.
- [23] R. Schmidt, R. Wüchner, and K.-U. Bletzinger. Isogeometric analysis of trimmed NURBS geometries. *Computer Methods in Applied Mechanics and Engineering*, 241–244:93–111, 2012.
- [24] M. A. Scott, D. C. Thomas, and E. J. Evans. Isogeometric spline forests. *Comp. Methods Appl. Mech. Engrg.*, 269:222–264, 2014.
- [25] T. W. Sederberg, G. T. Finnigan, X. Li, H. Lin, and H. Ipson. Watertight trimmed NURBS. *ACM Trans. Graphics*, 27(3):article no. 79, 2008.

- [26] Thomas W. Sederberg, David L. Cardon, G. Thomas Finnigan, Nicholas S. North, Jianmin Zheng, and Tom Lyche. T-spline simplification and local refinement. *ACM Trans. Graph.*, 23(3):276–283, 2004.
- [27] T. Takacs and B. Jüttler. Existence of stiffness matrix integrals for singularly parameterized domains in isogeometric analysis. *Computer Methods in Applied Mechanics and Engineering*, 200:3568–3582, 2011.
- [28] X. Yuan and W. Ma. Mapped B-spline basis functions for shape design and isogeometric analysis over an arbitrary parameterization. *Comp. Methods Appl. Mech. Engrg.*, 269:87–107, 2014.